Chapter 4
Multipole model of the Earth's magnetic field

Previously

- A measurement of the geomagnetic field at any given point and time consists of a superposition of fields from different sources:
  - Internal sources:
    - Core or main field: A hydrodynamic dynamo in the Earth's fluid outer core (2900 – 5100 km depth) produces over 99% of the Earth's magnetic field.
    - Crustal or anomalous or lithospheric field: The magnetic field caused by magnetized rocks in the lithosphere (< 50 km depth) can locally exceed the strength of the Earth's main field, but globally constitutes <1% of the field.
  - External sources:
    - Solar activity drives electric currents in the Earth's ionosphere and magnetosphere (> 100 km altitude) which cause irregular magnetic field variations with periods from seconds to hours.
- The first order approximation of the Earth's rather complex magnetic field is the dipole model.

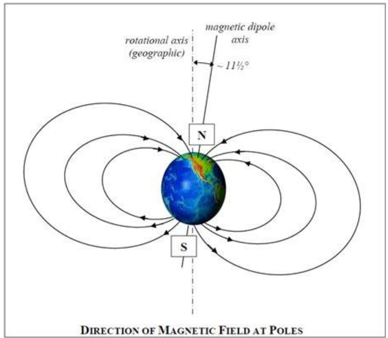

Content

- Spherical harmonic expansion of the Earth's magnetic field
- Properties of the spherical harmonic expansion
- International Geomagnetic Reference Field (IGRF)

Multipole model of the Earth's magnetic field

- Generalization of the dipole model of the Earth's magnetic field.
- Basic assumption: the Earth's magnetic field can be represented as a superposition of the fields created by several multipole magnets located at the center of the Earth.
- The simplest multipole magnet is the dipole, then quadrupole (four poles), octupole (eight poles), etc.

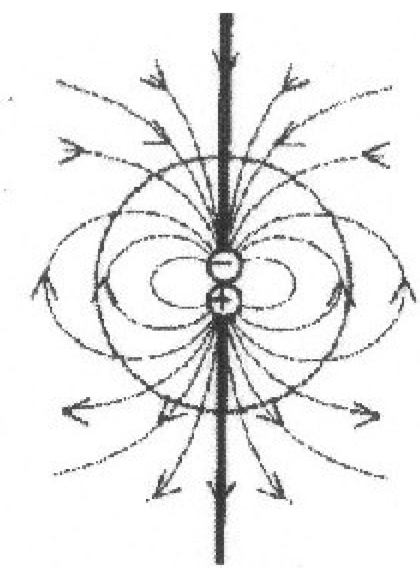

dipole

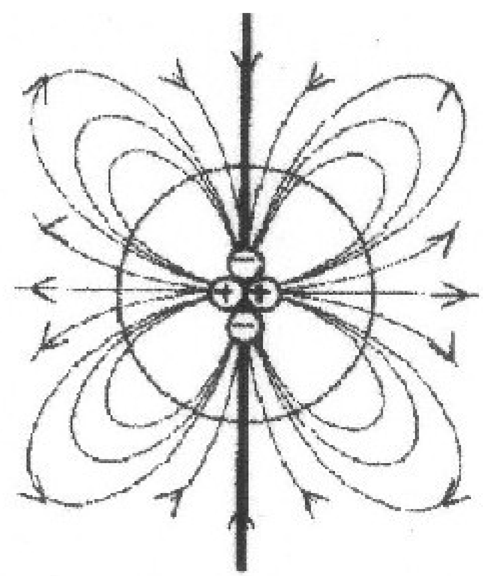

quadrupole

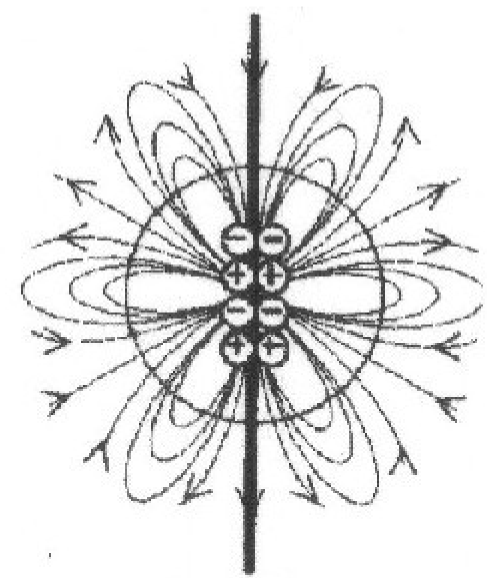

octupole

Spherical harmonics

- Spherical harmonics are a series of special functions defined on the surface of a sphere.
- As Fourier series are a series of functions used to represent functions on a circle, spherical harmonics are a series of functions that are used to represent functions defined on the surface of a sphere.
- Spherical harmonics are defined as the angular portion of a set of solutions to Laplace's equation in three dimensions.
- Spherical harmonics are functions defined in terms of spherical coordinates and and organized by wavelength.

$$Y_l^m(\theta,\varphi)=\sqrt{\frac{2l+1}{4\pi}\frac{(l-m)!}{(l+m)!}}\,P_l^m(\cos\theta)\,e^{im\varphi}$$

θ co-latitude
φ longitude
l degree of spherical harmonic
m order of spherical harmonic
$P_l^m(\cos\theta)$ associated Legendre function of the first kind

Legendre functions

The first few Legendre functions $P_n(x)$ are:

$P_0(x)=1$

$P_1(x)=x$

$P_2(x)=\frac{1}{2}(3\mathrm{x}^2-1)$

$P_3(x)=\frac{1}{2}(5\mathrm{x}^3-3\mathrm{x})$

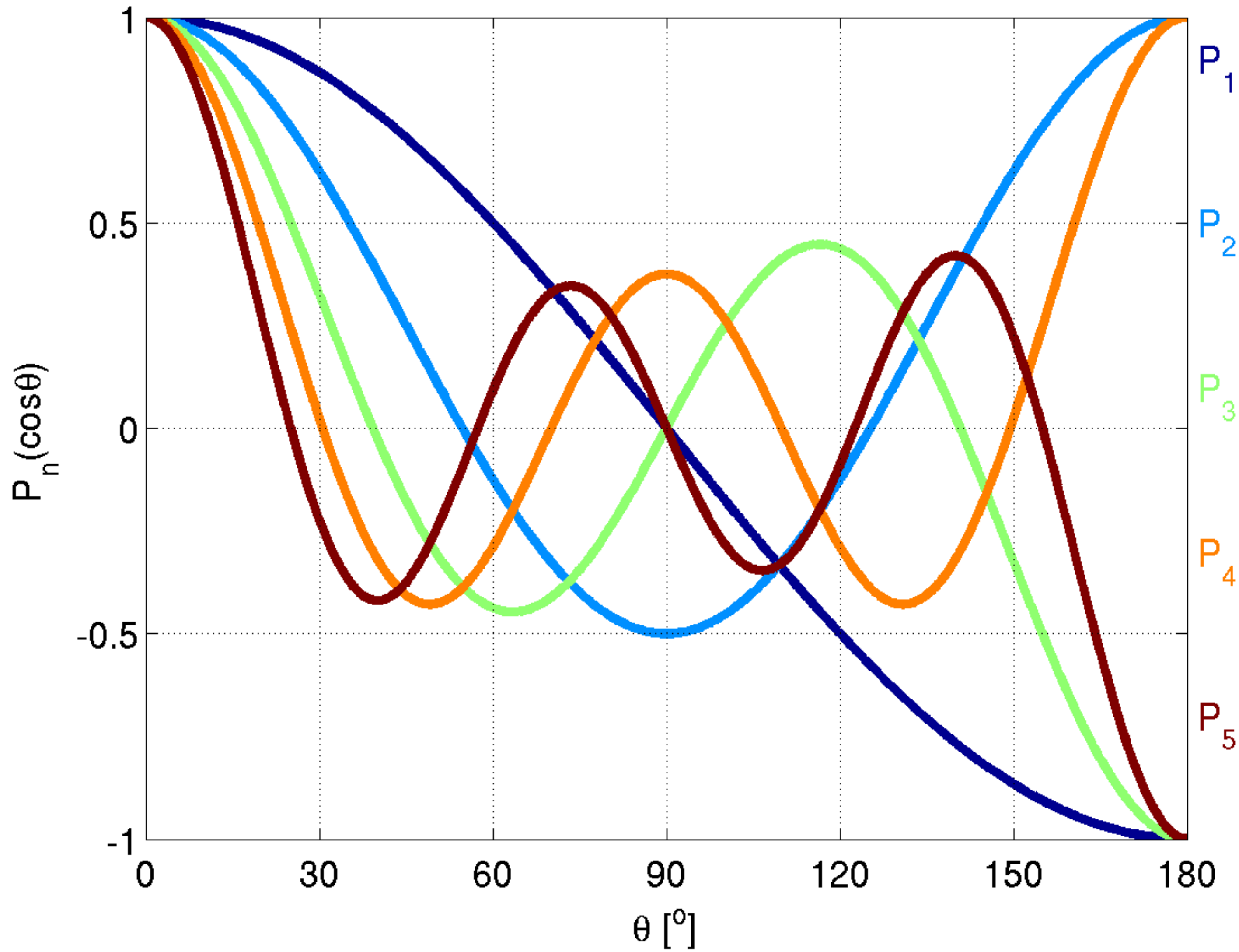

1
0.5
0
-0.5
-1
0
30
60
90
120
150
180
P_n(cosθ)
θ [°]
P_1
P_2
P_3
P_4
P_5

Unnormalized associated Legendre functions of the first kind

The unnormalized associated Legendre functions $P_n^m(x)$ are related to the Legendre functions $P_n(x)$ by:

$m=0$: $P_n^0(x)=P_n(x)$

$$m\neq 0:\ P_n^m(x)=(-1)^m(1-x^2)^{m/2}\frac{d^m}{dx^m}P_n(x)$$

Matlab function: P = legendre(n,x)

The first few unnormalized associated Legendre functions $P_n^m(x)$ are:

$$P_0^0(x)=1$$
$$P_1^0(x)=x$$
$$P_1^1(x)=-(1-x^2)^{1/2}$$
$$P_2^0(x)=\frac{1}{2}(3x^2-1)$$
$$P_2^1(x)=-3x(1-x^2)^{1/2}$$
$$P_2^2(x)=3(1-x^2)$$
$$P_3^0(x)=\frac{1}{2}(5x^3-3x)$$
$$P_3^1(x)=-\frac{3}{2}(5x^2-1)(1-x^2)^{1/2}$$
$$P_3^2(x)=15x(1-x^2)$$
$$P_3^3(x)=-15(1-x^2)^{3/2}$$

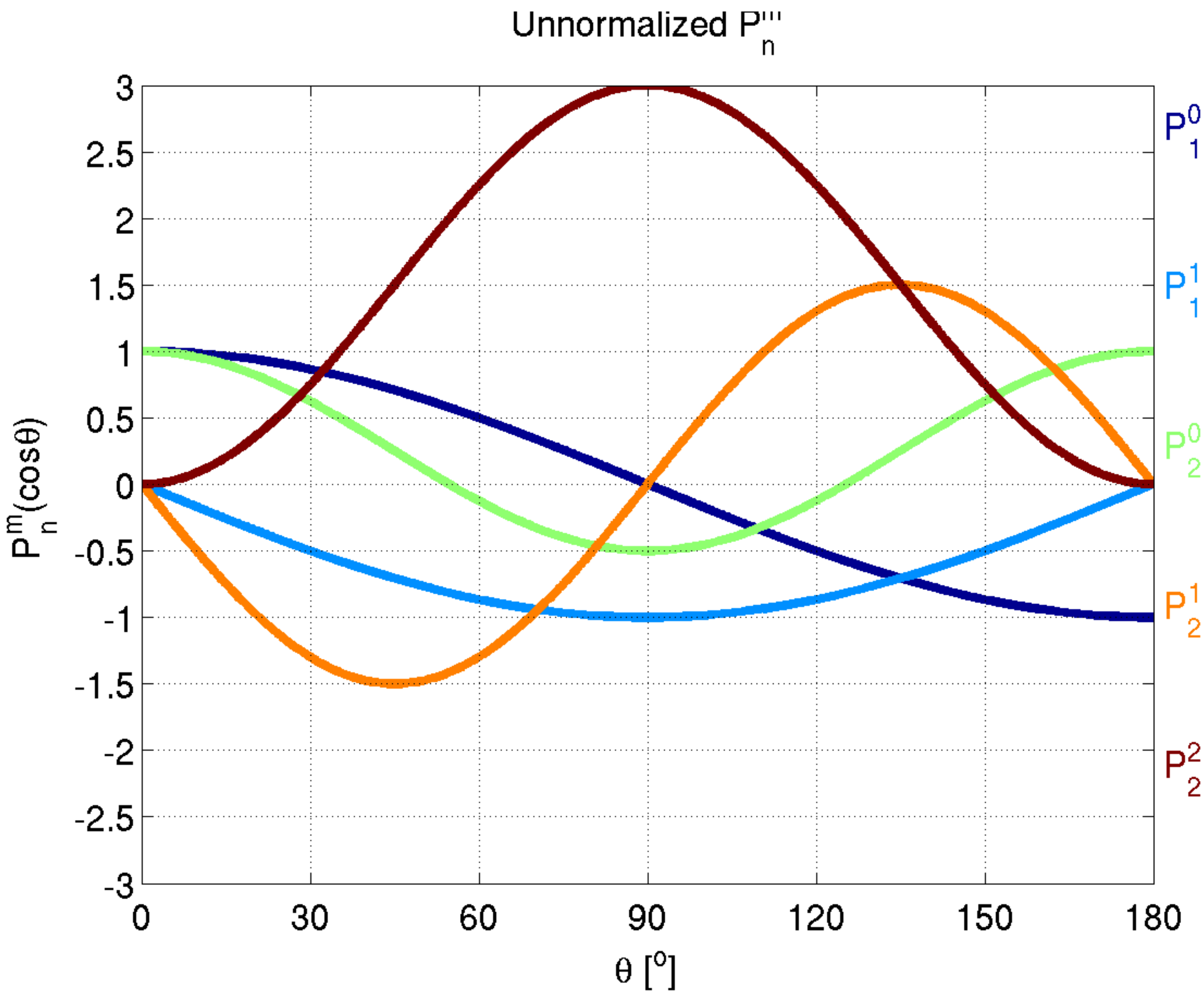

Unnormalized P
m
n
3
2.5
2
1.5
1
0.5
0
-0.5
-1
-1.5
-2
-2.5
-3
P
m
n
(cosθ)
0
30
60
90
120
150
180
θ [o]
P
0
1
P
1
1
P
0
2
P
1
2
P
2
2

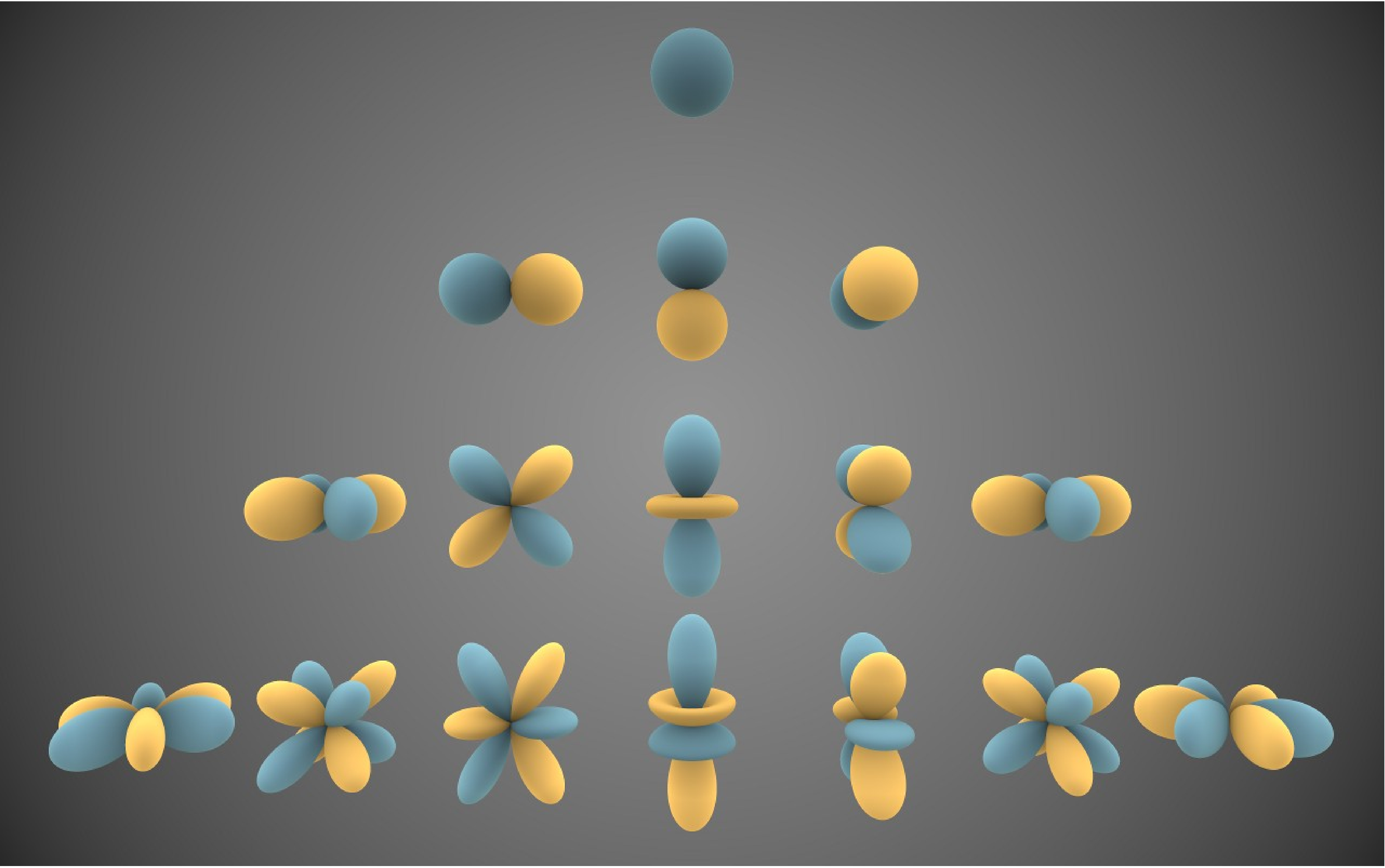

Visual representations of the first few real spherical harmonics. Blue portions represent regions where the function is positive, and yellow portions represent where it is negative. The distance of the surface from the origin indicates the value of $Y_l^m(\theta,\varphi)$ in angular direction (θ,φ).

Wavelength related to harmonic degree

- Spherical harmonics have
  - *n*-*m* zeros on parallels in π radians of co-latitude
  - *m* zeros on meridians in π radians of longitude.
- Spherical harmonics with $m = 0$ are called zonal, i.e., the functions are independent of the longitude φ.
- Spherical harmonics with $m = l$ are called sectorial, i.e., they represent bands of longitude.
- Spherical harmonics with $m \neq l \neq 0$ are called tesseral.

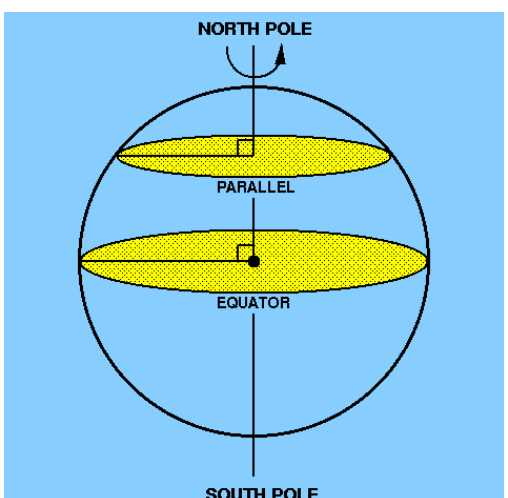

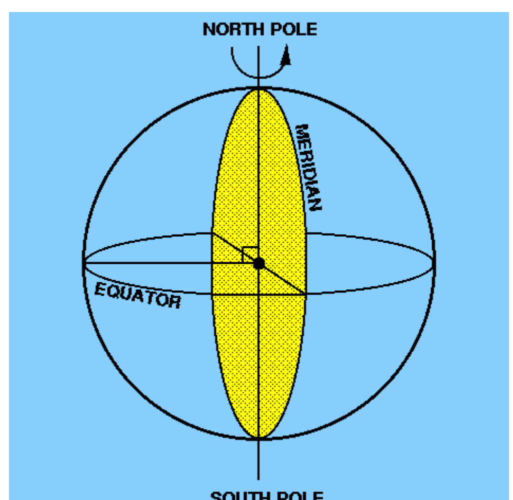

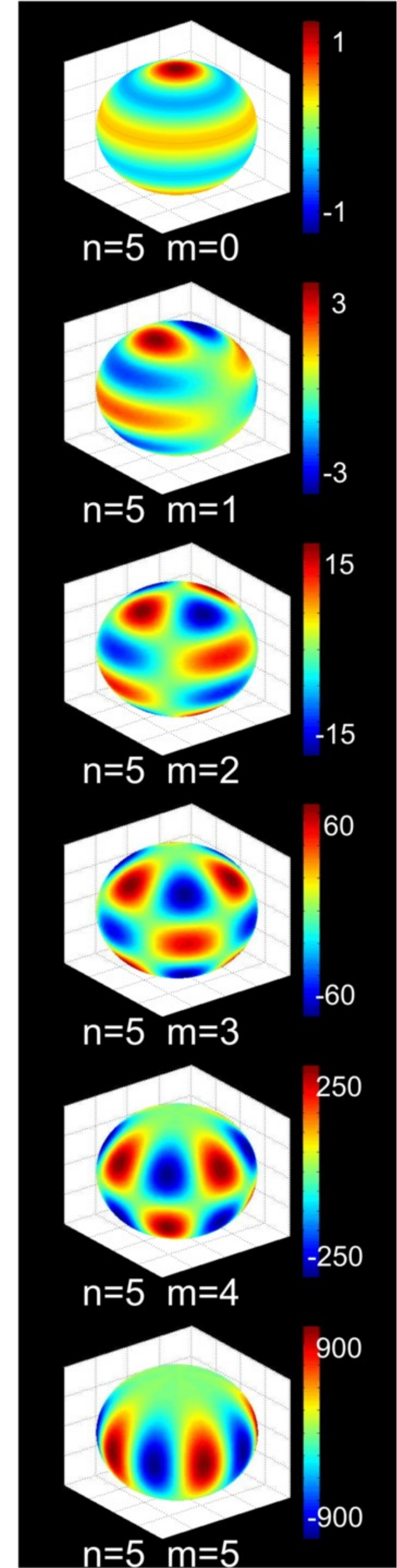

- Although the spherical harmonics are functions on a two-dimensional surface, it is sometimes convenient to characterize them by a one-dimensional "wavelength" λ. Since a spherical harmonic has n zeros on π radians, λ is taken to be:

$$\lambda = \frac{2\pi R_E \sin\theta}{n}$$

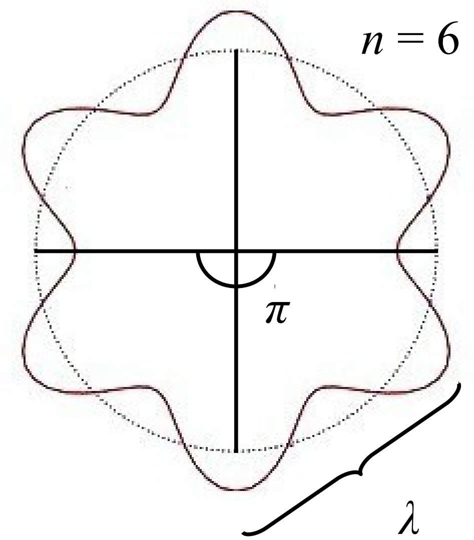

Laplace equation

$\nabla \times \boldsymbol{B} = 0 \rightarrow \boldsymbol{B} = -\nabla U$,
where U is the scalar potential.
$\nabla \cdot \boldsymbol{B} = 0 \rightarrow \nabla^2 U = 0$ (Laplace equation)

$$\nabla^2 U = \frac{1}{r^2}\frac{\partial}{\partial r}\left(r^2 \frac{\partial U}{\partial r}\right) + \frac{1}{r^2 \sin\theta}\frac{\partial}{\partial \theta}\left(\sin\theta \frac{\partial U}{\partial \theta}\right) + \frac{1}{r^2 \sin^2\theta}\frac{\partial^2}{\partial \varphi^2} = 0$$

There are two types of solutions:
- potential U_i due to sources internal to the Earth $(r < R_E)$
- potential U_e due to sources external to the Earth $(r > R_E)$

such that $U = U_i + U_e$.

The solutions are given as multipole or spherical harmonic expansions:

$$U_i(r,\theta,\varphi,t) = R_E \sum_{n=1}^{\infty} \left[\left(\frac{R_E}{r} \right)^{n+1} \sum_{m=0}^{n} \left(g_n^m(t) \cos m\varphi + h_n^m(t) \sin m\varphi \right) SP_n^m(\cos\theta) \right]$$

$$U_e(r,\theta,\varphi,t) = R_E \sum_{n=1}^{\infty} \left[\left(\frac{R_E}{r} \right)^{-n} \sum_{m=0}^{n} \left(q_n^m(t) \cos m\varphi + s_n^m(t) \sin m\varphi \right) SP_n^m(\cos\theta) \right]$$

r radius
R_E Earth radius $(R_E = 6371.2 \text{ km})$
θ co-latitude
φ longitude
t time
n degree of multipole (a multipole of degree n has 2^n poles)
m order of multipole
g, h, q, s spherical harmonic coefficients (describe the strength of the multipole magnet in nT)
$SP_n^m(\cos\theta)$ Schmidt semi-normalized associated Legendre function of the first kind

Schmidt semi-normalized associated Legendre functions

Schmidt semi-normalized associated Legendre functions $SP_n^m(x)$ are related to the unnormalized associated Legendre functions $P_n^m(x)$ by:

$$m=0:\ SP_n^0(x)=P_n^0(x)=P_n(x)$$

$$m\neq 0:\ SP_n^m(x)=(-1)^m\sqrt{\frac{2(n-m)!}{(n+m)!}}\,P_n^m(x)$$

Matlab function: P = legendre(n,x,'sch')

The first few Schmidt semi-normalized associated Legendre functions $SP_n^m(x)$ are:

$$SP_0^0(x)=1$$

$$SP_1^0(x)=x$$

$$SP_1^1(x)=(1-x^2)^{1/2}$$

$$SP_2^0(x)=\frac{1}{2}(3x^2-1)$$

$$SP_2^1(x)=\sqrt{3}\,x(1-x^2)^{1/2}$$

$$SP_2^2(x)=\frac{\sqrt{3}}{2}(1-x^2)$$

$$SP_3^0(x)=\frac{1}{2}(5x^3-3x)$$

$$SP_3^1(x)=\frac{\sqrt{6}}{4}(5x^2-1)(1-x^2)^{1/2}$$

$$SP_3^2(x)=\frac{\sqrt{15}}{2}x(1-x^2)$$

$$SP_3^3(x)=\frac{\sqrt{10}}{4}(1-x^2)^{3/2}$$

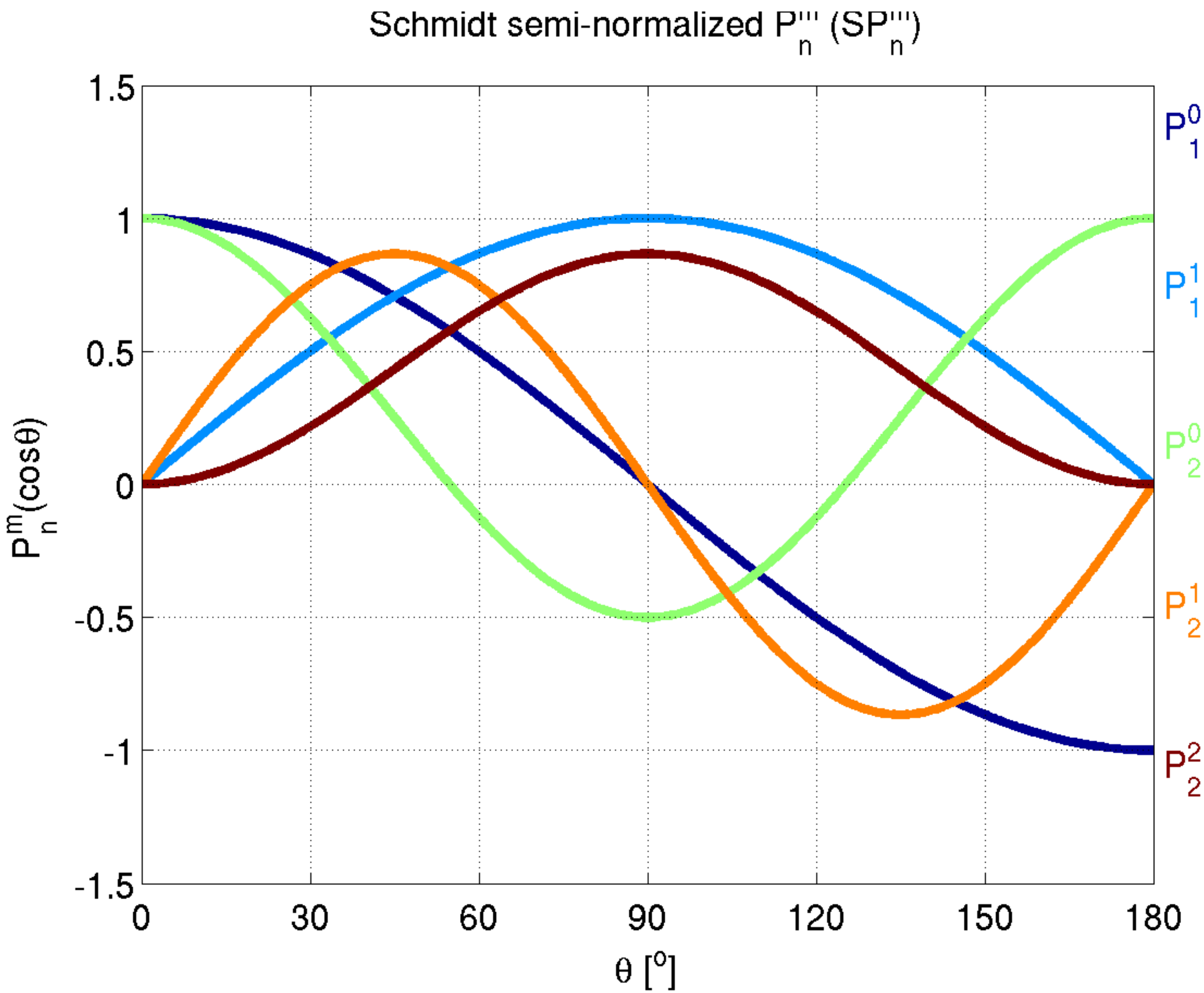
Schmidt semi-normalized P_n^m (SP_n^m)
1.5
1
0.5
0
-0.5
-1
-1.5
0
30
60
90
120
150
180
$P_n^m(\cos\theta)$
θ [^{o}]
P_1^0
P_1^1
P_2^0
P_2^1
P_2^2

Spherical harmonic expansion of the magnetic field

$$\boldsymbol{B}=-\nabla U=-\left(\frac{\partial U}{\partial r}\hat{\boldsymbol{e}}_r+\frac{1}{r}\frac{\partial U}{\partial \theta}\hat{\boldsymbol{e}}_\theta+\frac{1}{r\sin\theta}\frac{\partial U}{\partial \varphi}\hat{\boldsymbol{e}}_\varphi\right)$$

Sources internal to the Earth:

$$B_{r_i}(r,\theta,\varphi,t)=-\frac{\partial U_i}{\partial r}=\sum_{n=1}^{n_{max}}\left[(n+1)\left(\frac{R_E}{r}\right)^{n+2}\sum_{m=0}^{n}\left(g_n^m(t)\cos m\varphi+h_n^m(t)\sin m\varphi\right)SP_n^m(\cos\theta)\right]$$

$$B_{\theta_i}(r,\theta,\varphi,t)=-\frac{1}{r}\frac{\partial U_i}{\partial \theta}=-\sum_{n=1}^{n_{max}}\left[\left(\frac{R_E}{r}\right)^{n+2}\sum_{m=0}^{n}\left(g_n^m(t)\cos m\varphi+h_n^m(t)\sin m\varphi\right)\frac{dSP_n^m(\cos\theta)}{d\theta}\right]$$

$$B_{\varphi_i}(r,\theta,\varphi,t)=-\frac{1}{r\sin\theta}\frac{\partial U_i}{\partial \varphi}=-\sum_{n=1}^{n_{max}}\left[\left(\frac{R_E}{r}\right)^{n+2}\sum_{m=0}^{n}\left(-g_n^m(t)\sin m\varphi+h_n^m(t)\cos m\varphi\right)\frac{mSP_n^m(\cos\theta)}{\sin\theta}\right]$$

Sources external to the Earth:

$$B_{r_e}(r,\theta,\varphi,t)=-\frac{\partial U_e}{\partial r}=-\sum_{n=1}^{n_{max}}\left[n\left(\frac{R_E}{r}\right)^{-n+1}\sum_{m=0}^{n}\left(q_n^m(t)\cos m\varphi+s_n^m(t)\sin m\varphi\right)SP_n^m(\cos\theta)\right]$$

$$B_{\theta_e}(r,\theta,\varphi,t)=-\frac{1}{r}\frac{\partial U_e}{\partial \theta}=-\sum_{n=1}^{n_{max}}\left[\left(\frac{R_E}{r}\right)^{-n+1}\sum_{m=0}^{n}\left(q_n^m(t)\cos m\varphi+s_n^m(t)\sin m\varphi\right)\frac{dSP_n^m(\cos\theta)}{d\theta}\right]$$

$$B_{\varphi_e}(r,\theta,\varphi,t)=-\frac{1}{r\sin\theta}\frac{\partial U_e}{\partial \varphi}=-\sum_{n=1}^{n_{max}}\left[\left(\frac{R_E}{r}\right)^{-n+1}\sum_{m=0}^{n}\left(-q_n^m(t)\sin m\varphi+s_n^m(t)\cos m\varphi\right)\frac{mSP_n^m(\cos\theta)}{\sin\theta}\right]$$

- In practice, the sum to infinity has to be truncated at $n = n_{max}$, determined by the number of available observations.
- There are $n_{max}^2 + 2n_{max}$ coefficients in the expansion.
- In practice, the number of observations is generally much larger than this.
- The values of the coefficients are determined using the least squares method.

$\frac{d}{d\theta} SP_n^m(\cos\theta)$ from recurrence formulas

$m>0:$

$$(1-x^2)\frac{d}{dx}P_n^m(x)=(n+m)(n-m+1)\sqrt{1-x^2}\,P_n^{m-1}(x)+m\,x\,P_n^m(x)$$

$$\frac{d}{dx}SP_n^m(x)=(-1)^m\sqrt{\frac{2(n-m)!}{(n+m)!}}\frac{d}{dx}P_n^m(x)$$

$$\frac{d\,P_n^m(\cos\theta)}{d\theta}=\frac{d\cos\theta}{d\theta}\frac{d\,P_n^m(\cos\theta)}{d(\cos\theta)}=-\sin\theta\frac{d\,P_n^m(\cos\theta)}{d(\cos\theta)}$$

$m=0:$

$$(1-x^2)\frac{d}{dx}P_n(x)=nP_{n-1}(x)-nxP_n(x)$$

$$\frac{d}{dx}SP_n(x)=\frac{d}{dx}P_n(x)$$

$$\frac{d\,P_n(\cos\theta)}{d\theta}=\frac{d\cos\theta}{d\theta}\frac{d\,P_n(\cos\theta)}{d(\cos\theta)}=-\sin\theta\frac{d\,P_n(\cos\theta)}{d(\cos\theta)}$$

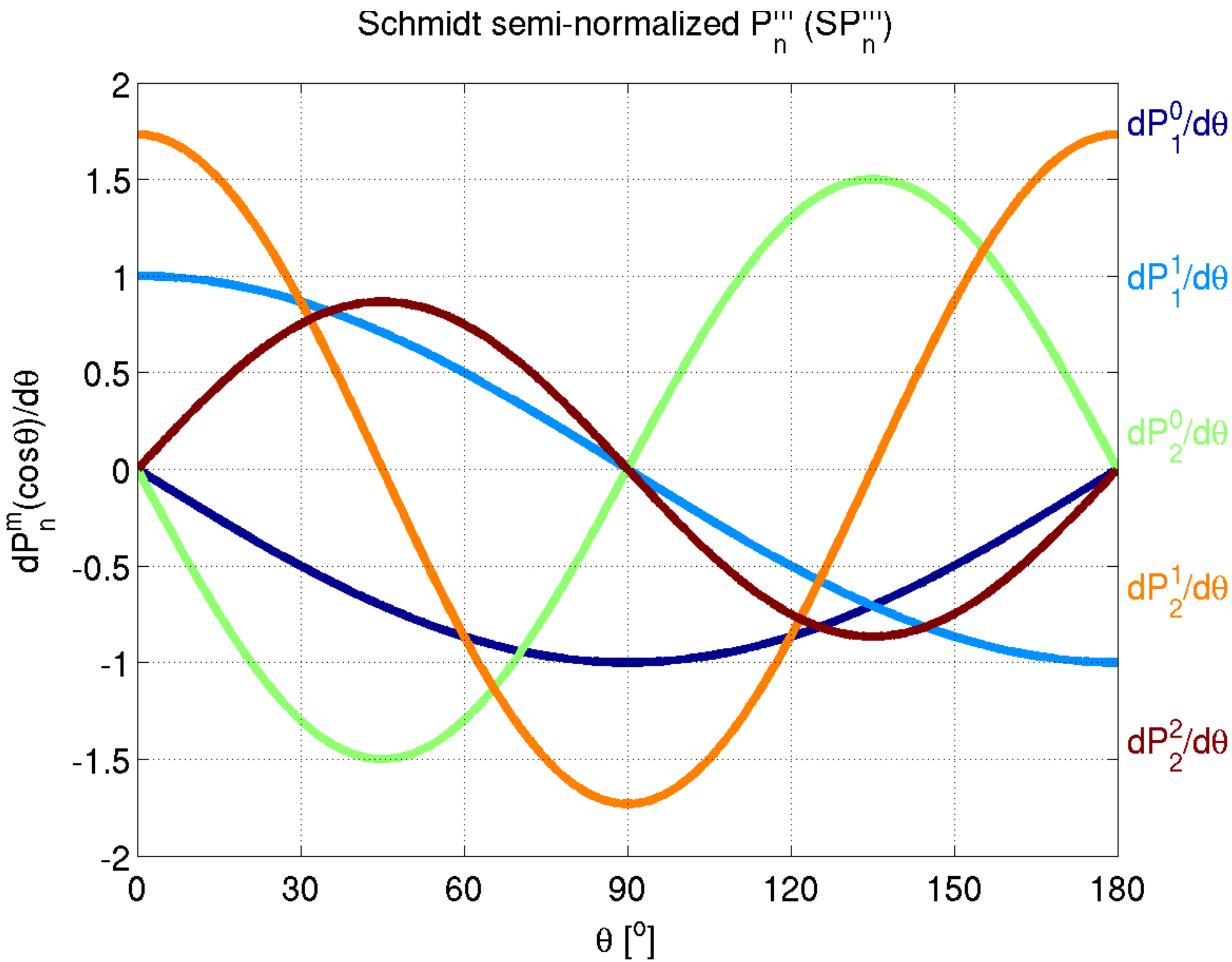

Schmidt semi-normalized P$_n^m$ (SP$_n^m$)
2
1.5
1
0.5
0
-0.5
-1
-1.5
-2
0
30
60
90
120
150
180
θ [°]
dP$_n^m$(cosθ)/dθ
dP$_1^0$/dθ
dP$_1^1$/dθ
dP$_2^0$/dθ
dP$_2^1$/dθ
dP$_2^2$/dθ

Properties of the spherical harmonic expansion

In case of the internal field:

- Large wavelengths ($n < 14$, approximately) are associated with the main field:
  - $n = 1$: dipole component
  - $2 \leq n < 14$: anomalous or non-dipole components

    (Note: The terms $2 \leq n < 14$ are considered anomalous relative to the dipole field whereas the terms $n > 14$ representing the crustal field are considered anomalous relative to the main field. Thus, the anomalous component is always relative, and the reference level should be mentioned.)
- Smaller wavelengths ($n > 14$) are associated with the magnetic anomalies of the crust.

Average magnetic field

In case of the magnetic field due to internal sources, the average of B_n^m squared over the Earth's surface S is defined as:

$$\langle (B_n^m)^2 \rangle = \frac{1}{4\pi} \oint (B_n^m)^2 \, dS$$

It can be shown that for each multipole (n) the result is:

$$\langle (B_n)^2 \rangle = (n+1) \sum_{m=0}^{n} (g_n^m)^2 + (h_n^m)^2$$

This formula can be used to estimate the relative strengths of the different multipoles:
(Model: POMME-6.2 2005.0)

n	1	2	3	4	5	6	7	8	9	10	11	12	13
$\frac{\sqrt{\langle (B_n)^2 \rangle}}{\sqrt{\langle (B_1)^2 \rangle}} \cdot 100$	100	20	15	7.3	3.3	1.5	0.9	0.4	0.3	0.1	0.1	0.0	0.0
$\frac{\sqrt{\langle (B_n)^2 \rangle}}{\sum_{n=1}^{N} \sqrt{\langle (B_n)^2 \rangle}} \cdot 100\%$	67	14	9.7	4.9	2.2	1.0	0.6	0.3	0.2	0.1	0.0	0.0	0.0

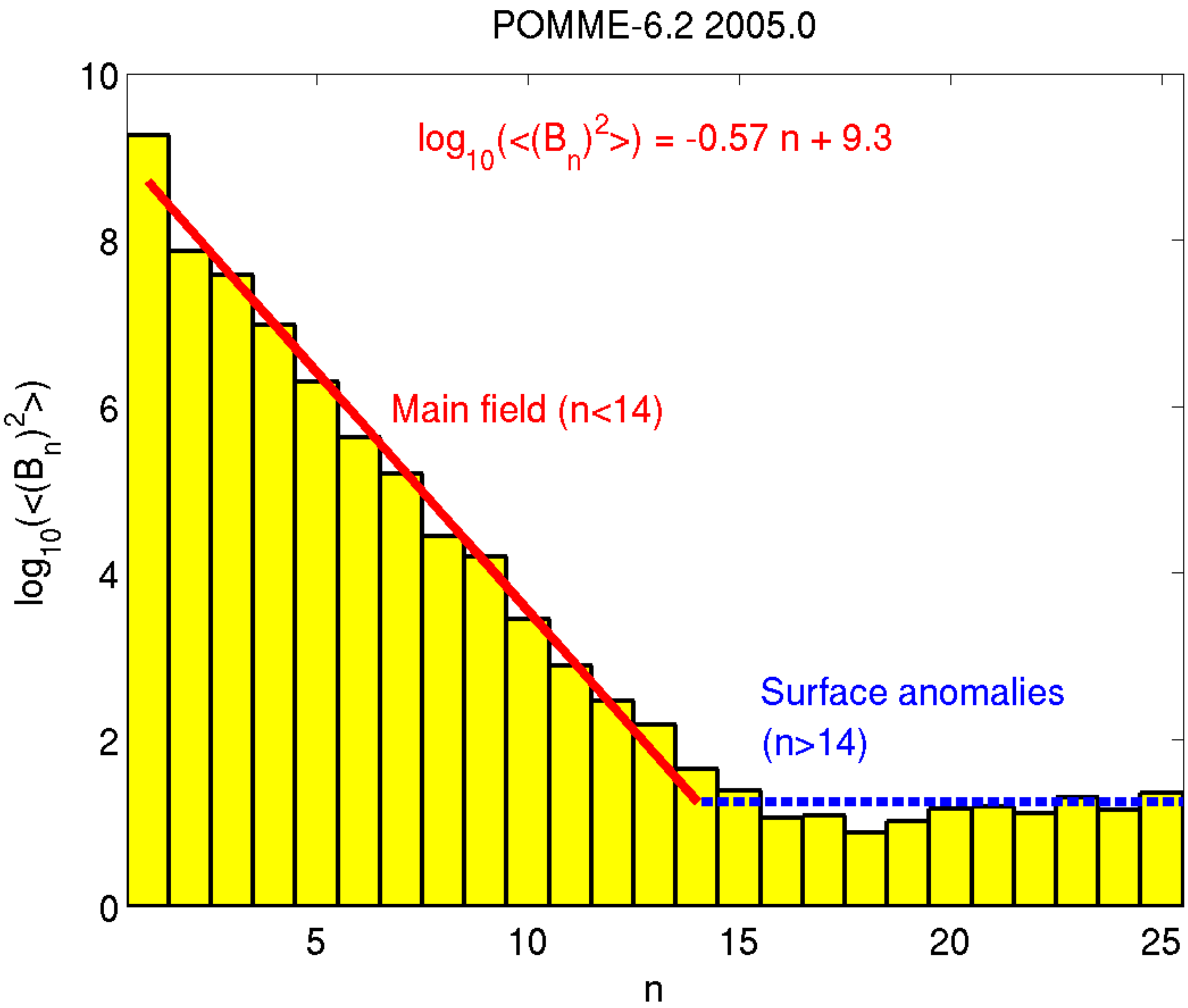
POMME-6.2 2005.0
log10(<(Bn)2>) = -0.57 n + 9.3
Main field (n<14)
Surface anomalies
(n>14)
log10(<(Bn)2>)
n
0
2
4
6
8
10
5
10
15
20
25

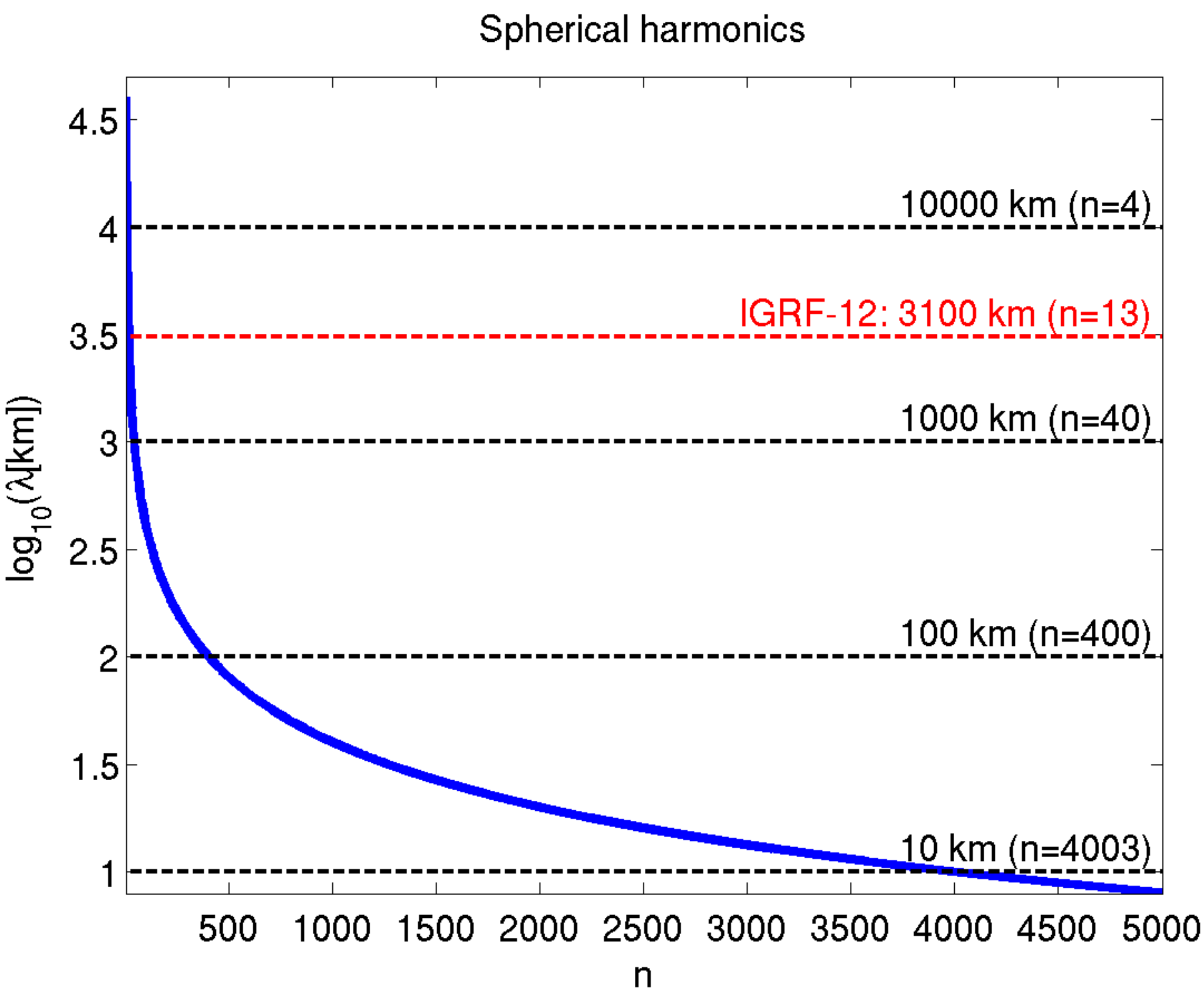

Minimum wavelength at the equator ($\theta = 90^{o}$) associated with the spherical harmonic of degree n.

If $r = R_C < R_E$ (source region of the magnetic field at the surface of the liquid core):

$$\langle (B_n)^2 \rangle_C = \left(\frac{R_E}{R_C} \right)^{2(n+2)} \langle (B_n)^2 \rangle_E$$

$$\rightarrow \log_{10}(\langle (B_n)^2 \rangle_E) = -2(n+2) \log_{10}(\frac{R_E}{R_C}) + \log_{10}(\langle (B_n)^2 \rangle_C)$$

$\rightarrow k = -\log_{10}(\frac{R_E}{R_C})^2 \approx -0.57$ (components $n < 14$ in the figure)

(Assume that $\log_{10}(\langle (B_n)^2 \rangle_C)$ does not depend on n.)

$$\rightarrow R_C = 10^{-\frac{0.57}{2}} R_E \approx 0.52 R_E \approx 3300 \text{ km}$$

When $R_C \rightarrow R_E, k \rightarrow 0$ (components $n > 14$ in the figure)

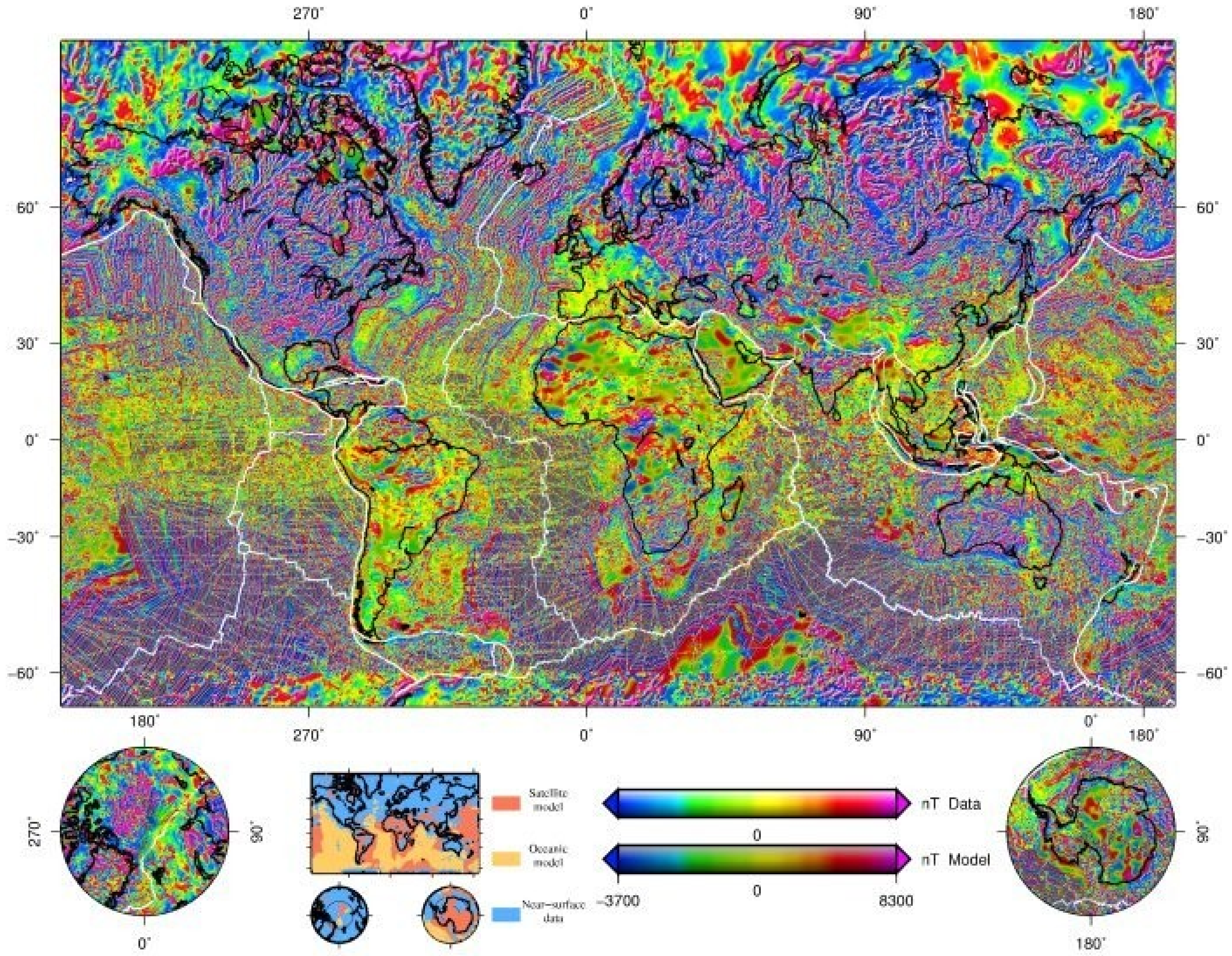

World Digital Anomaly Map (WDMAM 2007). Worldwide distribution of anomalies in the magnetic lithosphere.

International Geomagnetic Reference Field (IGRF)

http://www.ngdc.noaa.gov/IAGA/vmod/igrf.html

- Geomagnetic field models are represented as spherical harmonic expansions of a scalar magnetic potential. Such a model can then be evaluated at any desired location to provide the magnetic field vector.
- IGRF was introduced by the International Association of Geomagnetism and Aeronomy (IAGA) in 1968 in response to the demand for a standard spherical harmonic representation of the Earth's main field.
- IGRF can be considered to consist of two parts:
  - mathematical functions that describe how each multipole field changes as a function of latitude, longitude, and radius ("geometry of the multipole field")
  - coefficients ($2n+1$ for each $n \geq 1$) associated with each multipole ("strength of the multipole field")

- IGRF is meant to give a reasonable approximation, near and above the Earth's surface, to that part of the Earth's magnetic field which has its origin inside the surface.
- The model is updated at 5-year intervals. The latest (as of May 2015) is IGRF-12.
- At any one epoch, the IGRF specifies the numerical coefficients of a truncated spherical harmonic series.
  - For dates until 2000 the truncation is at n = 10, with 120 coefficients.
  - From 2000 the truncation is at n = 13, with 195 coefficients.
- Such a model is specified every 5 years, for epochs 1900.0, 1905.0, etc. For dates between the model epochs, coefficient values are given by linear interpolation.
- For the 5 years after the most recent epoch there is a linear secular variation model for forward extrapolation; this SV model is truncated at n = 8, so has 80 coefficients (in effect the next 40 or 115 coefficients are defined to be zero).

$$g_n^m(t) = g_n^m(t_0) + \boxed{g'^m_n(t_0)}(t - t_0) + g''^m_n(t_0)\frac{(t-t_0)^2}{2!} + \dots$$

$$h_n^m(t) = h_n^m(t_0) + \boxed{h'^m_n(t_0)}(t - t_0) + h''^m_n(t_0)\frac{(t-t_0)^2}{2!} + \dots$$

“Health warning”

- When using IGRF, to avoid ambiguity you should state explicitly which IGRF generation you are using.
- Because of the time variation of the field, really good models can only be produced for times when there is global coverage by satellites measuring the vector field. This occurred in:
  - 1979 – 1980: MAGSAT
  - 1999 – : Ørsted, CHAMP, SWARM
- At some time later, IGRF models are replaced by definitive DGRF models (“definitive = we will not be able to do significantly better in the future”).
- Interpolate between the appropriate DGRF models if they exist. If there is not a DGRF model, then use the appropriate IGRF model.
- If you measure the magnetic field at a point on the Earth's surface, do not expect to get the value predicted by the IGRF:
  - The numerical coefficients will not be correct: the model field produced will differ from the actual field.
  - Because of truncation, the IGRF model represents only the lower spatial frequencies (longer wavelengths) of the field: higher spatial frequency components are not accounted for.
  - There are also other contributions to the observed field (both natural and man-made) the IGRF is not trying to model: buildings, parked cars, magnetization of crustal rocks, traffic, DC electric trains and trams, electric currents in the ionosphere and magnetosphere, etc.

IGRF-12

- Full name: IGRF 12th generation
- Short name: IGRF-12
- Valid for: 1900.0 – 2020.0
- Definitive for: 1945.0 – 2010.0
- Reference: Thébault et al., Earth Planets and Space, 2015

Table 3 12th Generation International Geomagnetic Reference Field

	Degree	Order	IGRF	IGRF	IGRF	IGRF	IGRF	IGRF	IGRF	IGRF	IGRF	DGRF	DGRF	DGRF	DGRF	DGRF	DGRF	DGRF	DGRF	DGRF	DGRF	DGRF	DGRF	DGRF	DGRF	IGRF	SV
g/h	n	m	1900.0	1905.0	1910.0	1915.0	1920.0	1925.0	1930.0	1935.0	1940.0	1945.0	1950.0	1955.0	1960.0	1965.0	1970.0	1975.0	1980.0	1985.0	1990.0	1995.0	2000.0	2005.0	2010.0	2015	2015-20
g	1	0	-31543	-31464	-31354	-31212	-31060	-30926	-30805	-30715	-30654	-30594	-30554	-30500	-30421	-30334	-30220	-30100	-29992	-29873	-29775	-29692	-29619.4	-29554.63	-29496.57	-29442.0	10.3
g	1	1	-2298	-2298	-2297	-2306	-2317	-2318	-2316	-2306	-2292	-2285	-2250	-2215	-2169	-2119	-2068	-2013	-1956	-1905	-1848	-1784	-1728.2	-1669.05	-1586.42	-1501.0	18.1
h	1	1	5922	5909	5898	5875	5845	5817	5808	5812	5821	5810	5815	5820	5791	5776	5737	5675	5604	5500	5406	5306	5186.1	5077.99	4944.26	4797.1	-26.6
g	2	0	-677	-728	-769	-802	-839	-893	-951	-1018	-1106	-1244	-1341	-1440	-1555	-1662	-1781	-1902	-1997	-2072	-2131	-2200	-2267.7	-2337.24	-2396.06	-2445.1	-8.7
g	2	1	2905	2928	2948	2956	2959	2969	2980	2984	2981	2990	2998	3003	3002	2997	3000	3010	3027	3044	3059	3070	3068.4	3047.69	3026.34	3012.9	-3.3
h	2	1	-1061	-1086	-1128	-1191	-1259	-1334	-1424	-1520	-1614	-1702	-1810	-1898	-1967	-2016	-2047	-2067	-2129	-2197	-2279	-2366	-2481.6	-2594.50	-2708.54	-2845.6	-27.4
g	2	2	924	1041	1176	1309	1407	1471	1517	1550	1566	1578	1576	1581	1590	1594	1611	1632	1663	1687	1686	1681	1670.9	1657.76	1668.17	1676.7	2.1
h	2	2	1121	1065	1000	917	823	728	644	586	528	477	381	291	206	114	25	-68	-200	-306	-373	-413	-458.0	-515.43	-575.73	-641.9	-14.1
g	3	0	1022	1037	1058	1084	1111	1140	1172	1206	1240	1282	1297	1302	1302	1297	1287	1276	1281	1296	1314	1335	1339.6	1336.30	1339.85	1350.7	3.4
g	3	1	-1469	-1494	-1524	-1559	-1600	-1645	-1692	-1740	-1790	-1834	-1889	-1944	-1992	-2038	-2091	-2144	-2180	-2208	-2239	-2267	-2288.0	-2305.83	-2326.54	-2352.3	-5.5
h	3	1	-330	-357	-389	-421	-445	-462	-480	-494	-499	-499	-476	-462	-414	-404	-366	-333	-336	-310	-284	-262	-227.6	-198.86	-160.40	-115.3	8.2
g	3	2	1256	1239	1223	1212	1205	1202	1205	1215	1232	1255	1274	1288	1289	1292	1278	1260	1251	1247	1248	1249	1252.1	1246.39	1232.10	1225.6	-0.7
h	3	2	3	34	62	84	103	119	133	146	163	186	206	216	224	240	251	262	271	284	293	302	293.4	269.72	251.75	244.9	-0.4
g	3	3	572	635	705	778	839	881	907	918	916	913	896	882	878	856	838	830	833	829	802	759	714.5	672.51	633.73	582.0	-10.1
h	3	3	523	480	425	360	293	229	166	101	43	-11	-46	-83	-130	-165	-196	-223	-252	-297	-352	-427	-491.1	-524.72	-537.03	-538.4	1.8
g	4	0	876	880	884	887	889	891	896	903	914	944	954	958	957	957	952	946	938	936	939	940	932.3	920.55	912.66	907.6	-0.7
g	4	1	628	643	660	678	695	711	727	744	762	776	792	796	800	804	800	791	782	780	780	780	786.8	797.96	808.97	813.7	0.2
h	4	1	195	203	211	218	220	216	205	188	169	144	136	133	135	148	167	191	212	232	247	262	272.6	282.07	286.48	283.3	-1.3
g	4	2	660	653	644	631	616	601	584	565	550	544	528	510	504	479	461	438	398	361	325	290	250.0	210.65	166.58	120.4	-9.1
h	4	2	-69	-77	-90	-109	-134	-163	-195	-226	-252	-276	-278	-274	-278	-269	-266	-265	-257	-249	-240	-236	-231.9	-225.23	-211.03	-188.7	5.3
g	4	3	-361	-380	-400	-416	-424	-426	-422	-415	-405	-421	-408	-397	-394	-390	-395	-405	-419	-424	-423	-418	-403.0	-379.86	-356.83	-334.9	4.1
h	4	3	-210	-201	-189	-173	-153	-130	-109	-90	-72	-55	-37	-23	3	13	26	39	53	69	84	97	119.8	145.15	164.46	180.9	2.9
g	4	4	134	146	160	178	199	217	234	249	265	304	303	290	269	252	234	216	199	170	141	122	111.3	100.00	89.40	70.4	-4.3
h	4	4	-75	-65	-55	-51	-57	-70	-90	-114	-141	-178	-210	-230	-255	-269	-279	-288	-297	-297	-299	-306	-303.8	-305.36	-309.72	-329.5	-5.2
g	5	0	-184	-192	-201	-211	-221	-230	-237	-241	-241	-253	-240	-229	-222	-219	-216	-218	-218	-214	-214	-214	-218.8	-227.00	-230.87	-232.6	-0.2
g	5	1	328	328	327	327	326	326	327	329	334	346	349	360	362	358	359	356	357	355	353	352	351.4	354.41	357.29	360.1	0.5
h	5	1	-210	-193	-172	-148	-122	-96	-72	-51	-33	-12	3	15	16	19	26	31	46	47	46	46	43.8	42.72	44.58	47.3	0.6
g	5	2	264	259	253	245	236	226	218	211	208	194	211	230	242	254	262	264	261	253	245	235	222.3	208.95	200.26	192.4	-1.3
h	5	2	53	56	57	58	58	58	60	64	71	95	103	110	125	128	139	148	150	150	154	165	171.9	180.25	189.01	197.0	1.7
g	5	3	5	-1	-9	-16	-23	-28	-32	-33	-33	-20	-20	-23	-26	-31	-42	-59	-74	-93	-109	-118	-130.4	-136.54	-141.05	-140.9	-0.1
h	5	3	-33	-32	-33	-34	-38	-44	-53	-64	-75	-67	-87	-98	-117	-126	-139	-152	-151	-154	-153	-143	-133.1	-123.45	-118.06	-119.3	-1.2
g	5	4	-86	-93	-102	-111	-119	-125	-131	-136	-141	-142	-147	-152	-156	-157	-160	-159	-162	-164	-165	-166	-168.6	-168.05	-163.17	-157.5	1.4
h	5	4	-124	-125	-126	-126	-125	-122	-118	-115	-113	-119	-122	-121	-114	-97	-91	-83	-78	-75	-69	-55	-39.3	-19.57	-0.01	16.0	3.4
g	5	5	-16	-26	-38	-51	-62	-69	-74	-76	-76	-82	-76	-69	-63	-62	-56	-49	-48	-46	-36	-17	-12.9	-13.55	-8.03	4.1	3.9
h	5	5	3	11	21	32	43	51	58	64	69	82	80	78	81	81	83	88	92	95	97	107	106.3	103.85	101.04	100.2	0.0
g	6	0	63	62	62	61	61	61	60	59	57	59	54	47	46	45	43	45	48	53	61	68	72.3	73.60	72.78	70.0	-0.3
g	6	1	61	60	58	57	55	54	53	53	54	57	57	57	58	61	64	66	66	65	65	67	68.2	69.56	68.69	67.7	-0.1
h	6	1	-9	-7	-5	-2	0	3	4	4	4	6	-1	-9	-10	-11	-12	-13	-15	-16	-16	-17	-17.4	-20.33	-20.90	-20.8	0.0
g	6	2	-11	-11	-11	-10	-10	-9	-9	-8	-7	6	4	3	1	8	15	28	42	51	59	68	74.2	76.74	75.92	72.7	-0.7
h	6	2	83	86	89	93	96	99	102	104	105	100	99	96	99	100	100	99	93	88	82	72	63.7	54.75	44.18	33.2	-2.1
g	6	3	-217	-221	-224	-228	-233	-238	-242	-246	-249	-246	-247	-247	-237	-228	-212	-198	-192	-185	-178	-170	-160.9	-151.34	-141.40	-129.9	2.1
h	6	3	2	4	5	8	11	14	19	25	33	16	33	48	60	68	72	75	71	69	69	67	65.1	63.63	61.54	58.9	-0.7
g	6	4	-58	-57	-54	-51	-46	-40	-32	-25	-18	-25	-16	-8	-1	4	2	1	4	4	3	-1	-5.9	-14.58	-22.83	-28.9	-1.2
h	6	4	-35	-32	-29	-26	-22	-18	-16	-15	-15	-9	-12	-16	-20	-32	-37	-41	-43	-48	-52	-58	-61.2	-63.53	-66.26	-66.7	0.2
g	6	5	59	57	54	49	44	39	32	25	18	21	12	7	-2	1	3	6	14	16	18	19	16.9	14.58	13.10	13.2	0.3
h	6	5	36	32	28	23	18	13	8	4	0	-16	-12	-12	-11	-8	-6	-4	-2	-1	1	1	0.7	0.24	3.02	7.3	0.9
g	6	6	-90	-92	-95	-98	-101	-103	-104	-106	-107	-104	-105	-107	-113	-111	-112	-111	-108	-102	-96	-93	-90.4	-86.36	-78.09	-70.9	1.6
h	6	6	-69	-67	-65	-62	-57	-52	-46	-40	-33	-39	-30	-24	-17	-7	1	11	17	21	24	36	43.8	50.94	55.40	62.6	1.0
g	7	0	70	70	71	72	73	73	74	74	74	70	65	65	67	75	72	71	72	74	77	77	79.0	79.88	80.44	81.6	0.3
g	7	1	-55	-54	-54	-54	-54	-54	-54	-53	-53	-40	-55	-56	-56	-57	-57	-56	-59	-62	-64	-72	-74.0	-74.46	-75.00	-76.1	-0.2
h	7	1	-45	-46	-47	-48	-49	-50	-51	-52	-52	-45	-35	-50	-55	-61	-70	-77	-82	-83	-80	-69	-64.6	-61.14	-57.80	-54.1	0.8
g	7	2	0	0	1	2	2	3	4	4	4	0	2	2	5	4	1	1	2	3	2	1	0.0	-1.65	-4.55	-6.8	-0.5

Magnetic maps of the Earth

from
http://www.geomag.bgs.ac.uk/education/earthmag.html

Map of declination (degrees east or west of true north) at 2015.0

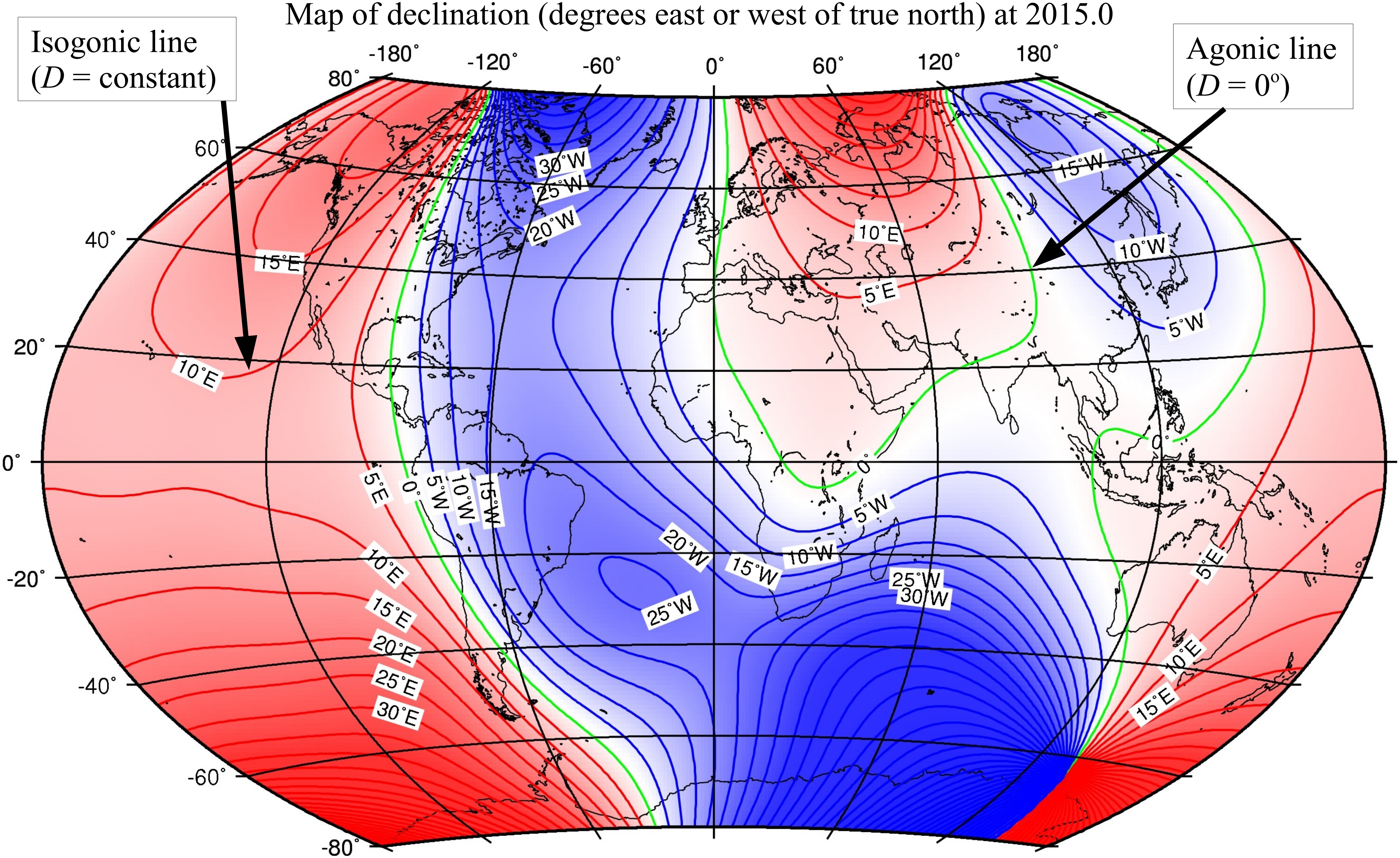

Map of predicted annual rate of change of declination (degrees/year east or west) for 2015.0-2020.0

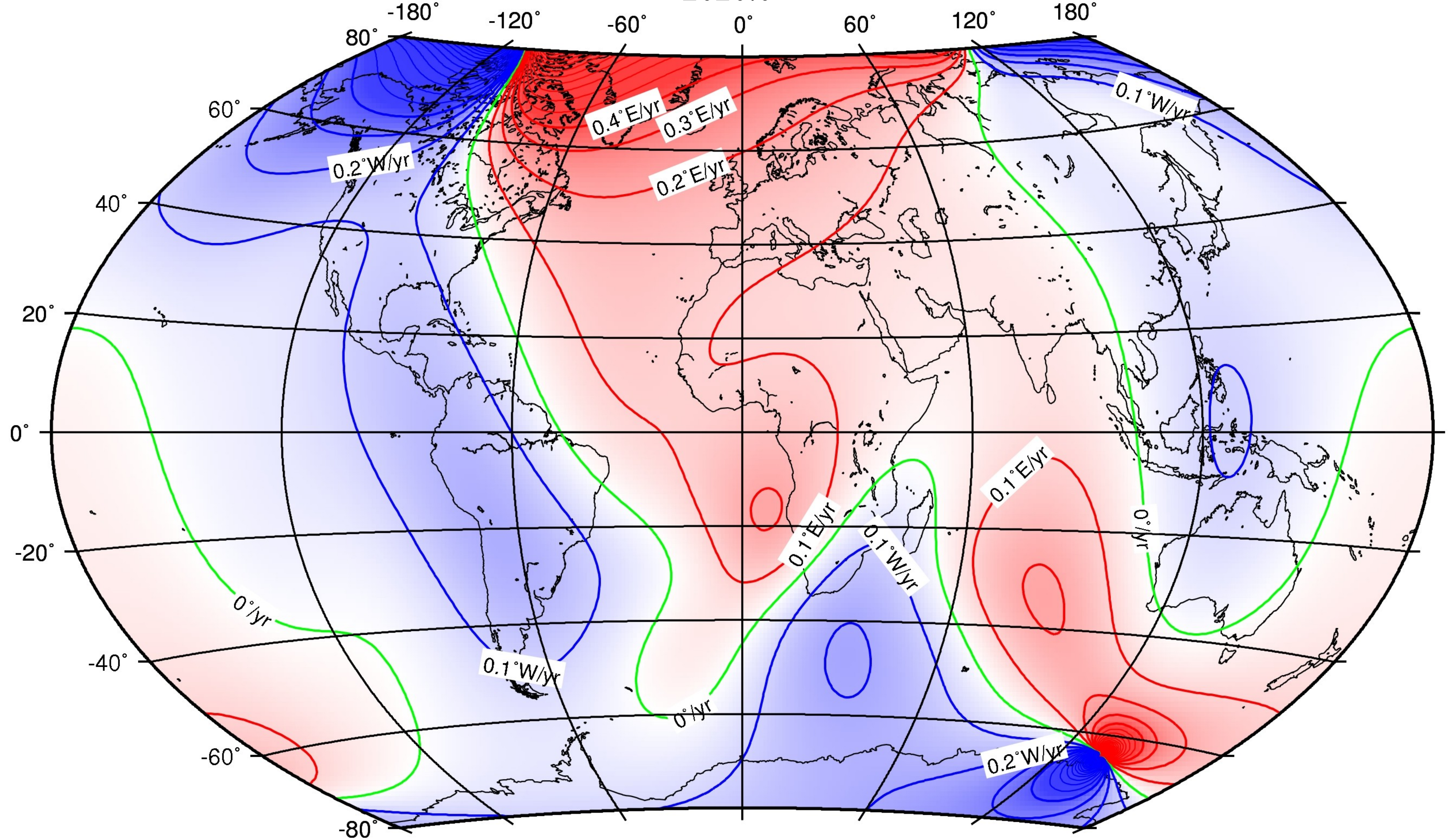

Map of inclination (angle in degrees up or down that magnetic field vector is from the horizontal) at 2015.0

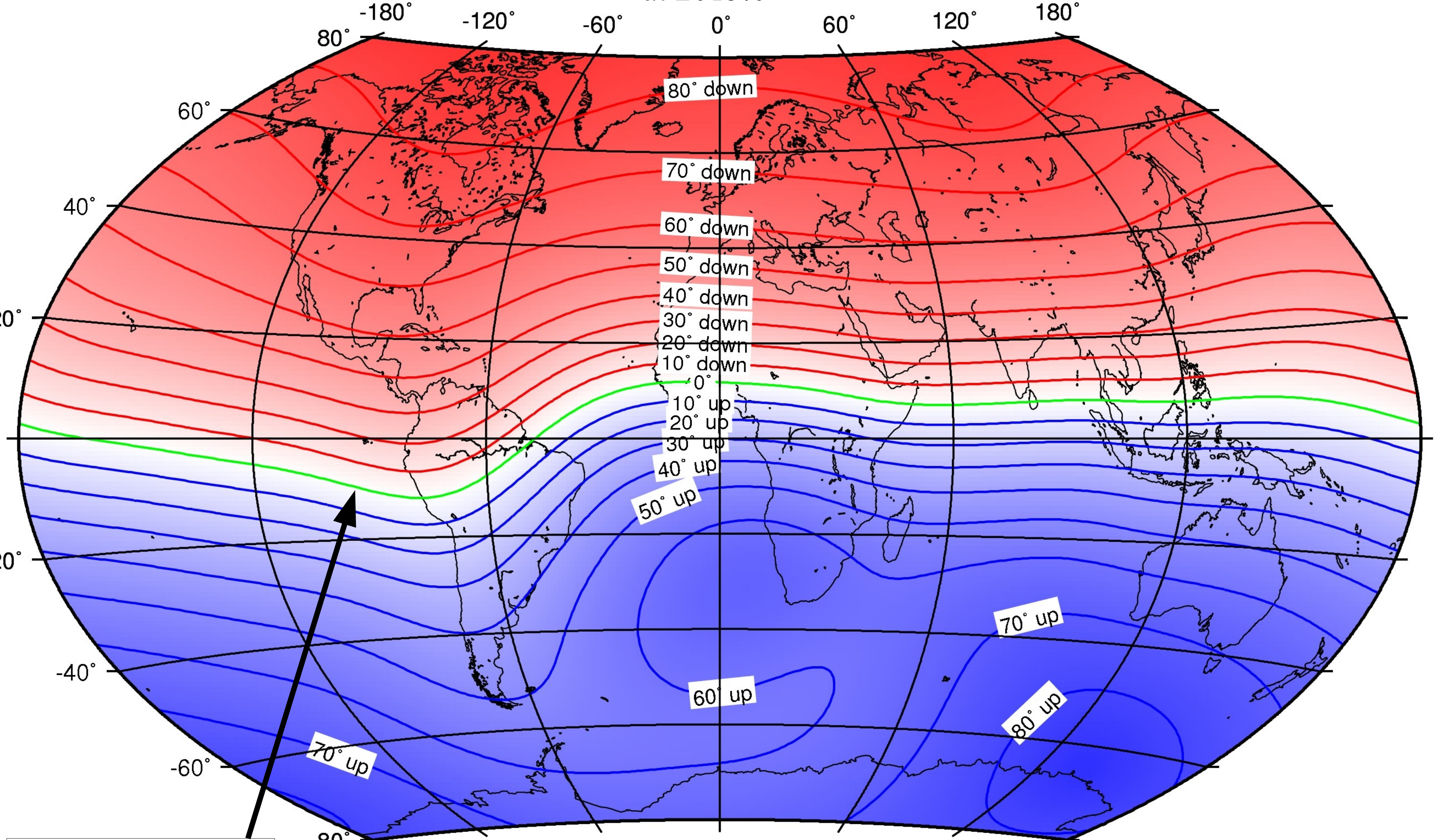

Magnetic equator ($I = 0^{o}$)

Map of predicted annual rate of change of inclination (degrees/year up or down) for 2015.0-2020.0

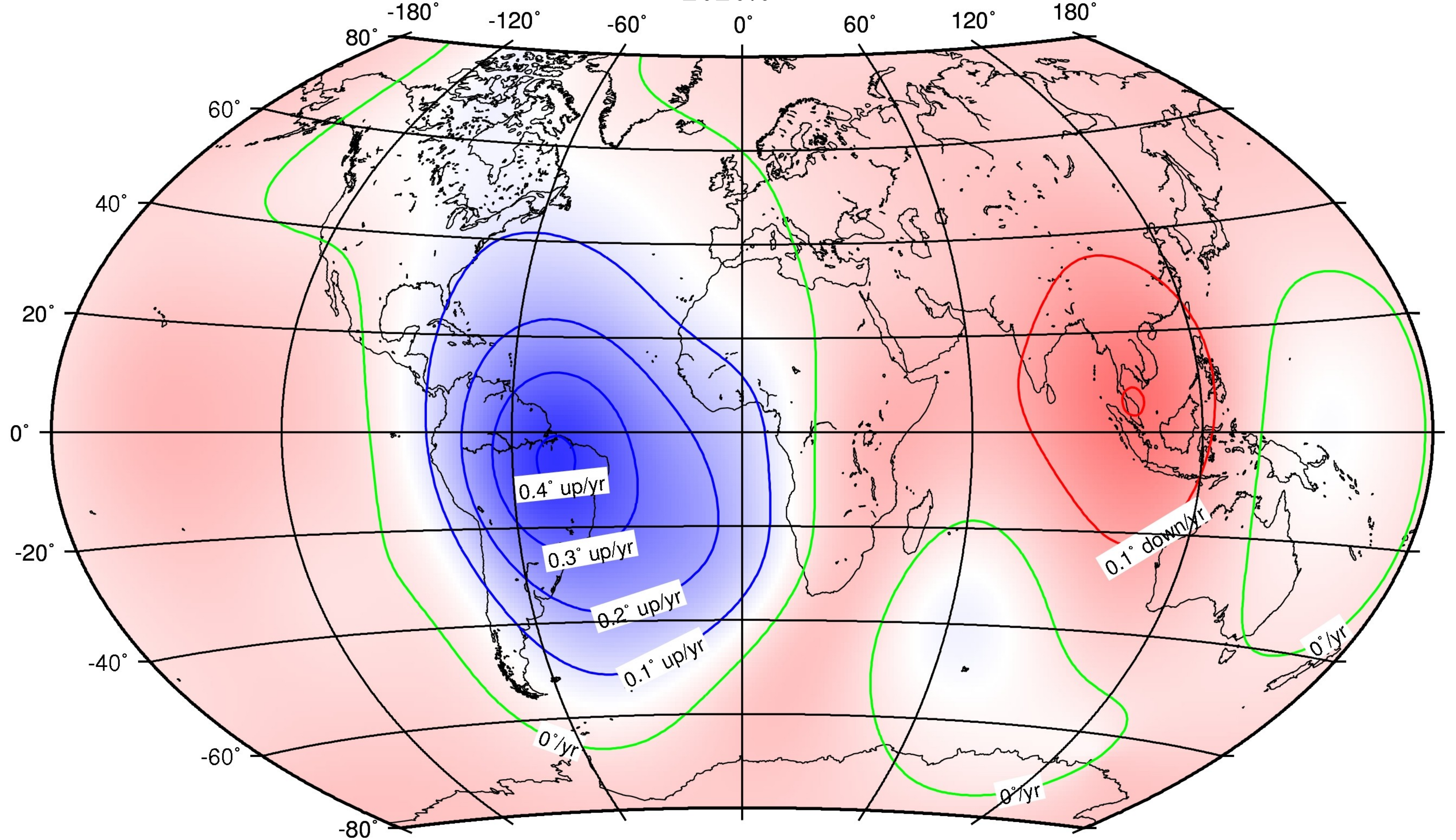

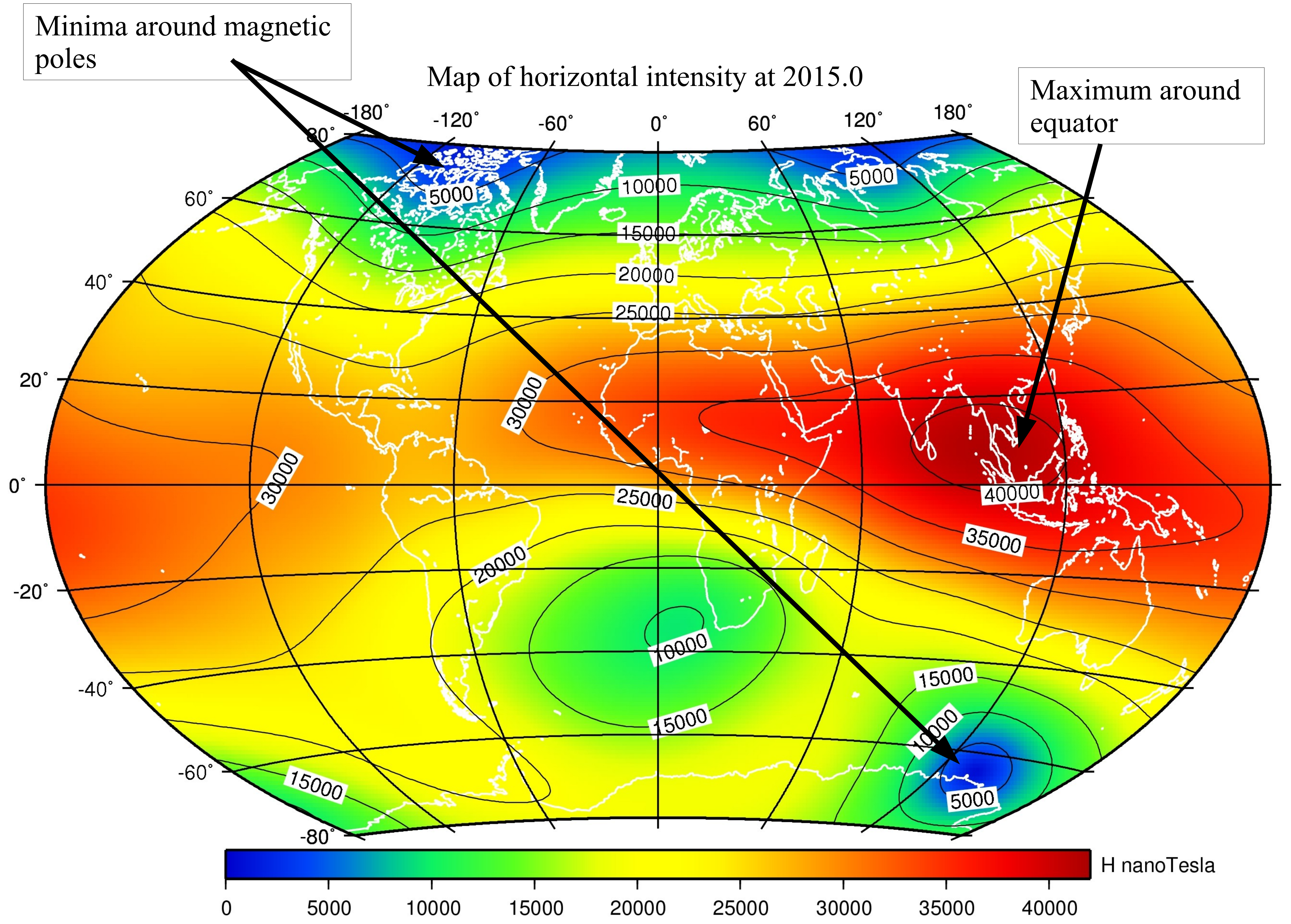

Minima around magnetic poles
Map of horizontal intensity at 2015.0
Maximum around equator
-180˚
-120˚
-60˚
0˚
60˚
120˚
180˚
80˚
60˚
40˚
20˚
0˚
-20˚
-40˚
-60˚
-80˚
5000
10000
15000
20000
25000
30000
35000
40000
H nanoTesla
0
5000
10000
15000
20000
25000
30000
35000
40000

Map of predicted annual rate of change of horizontal intensity for 2015.0-2020.0

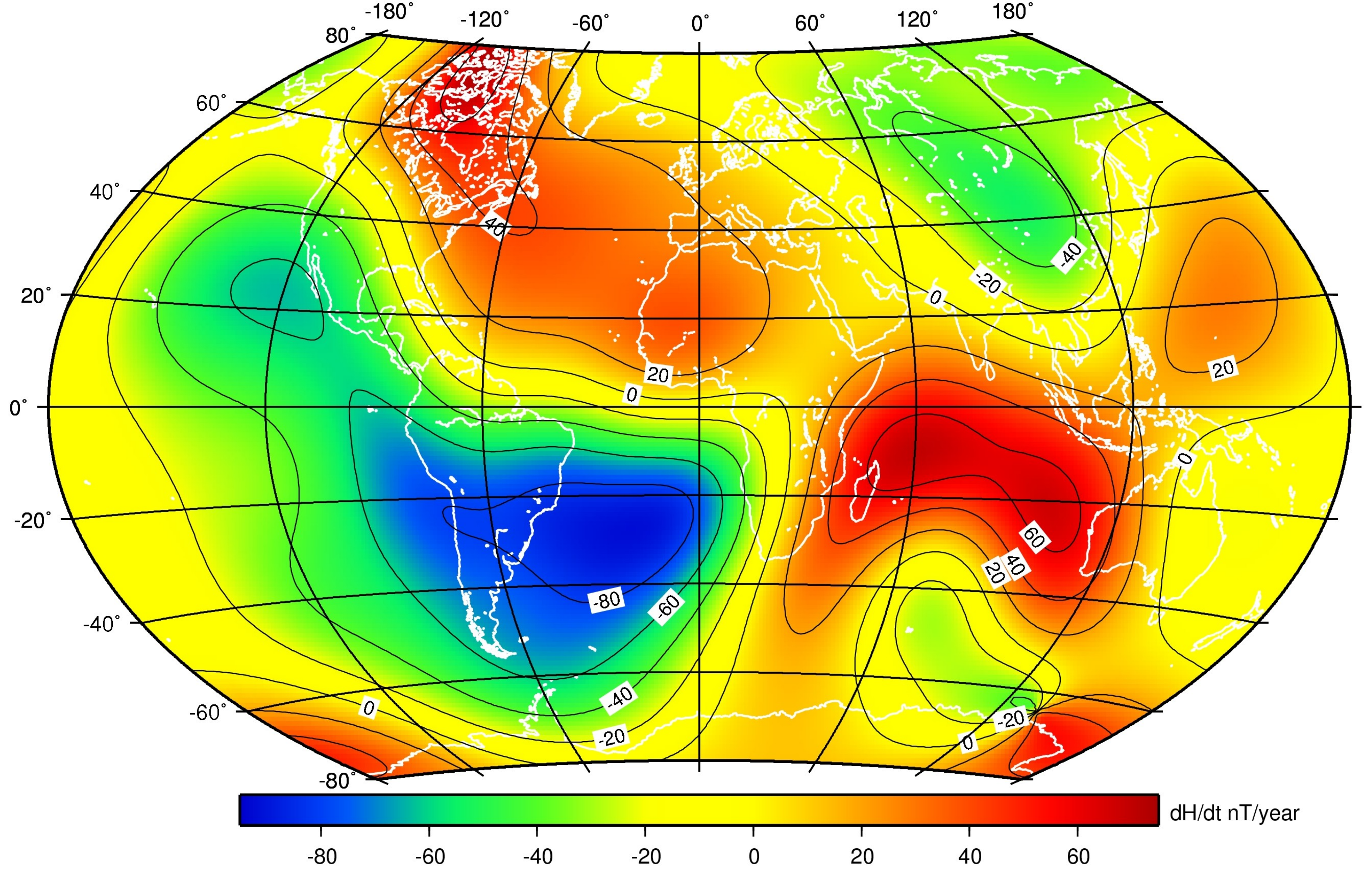

Map of vertical intensity at 2015.0

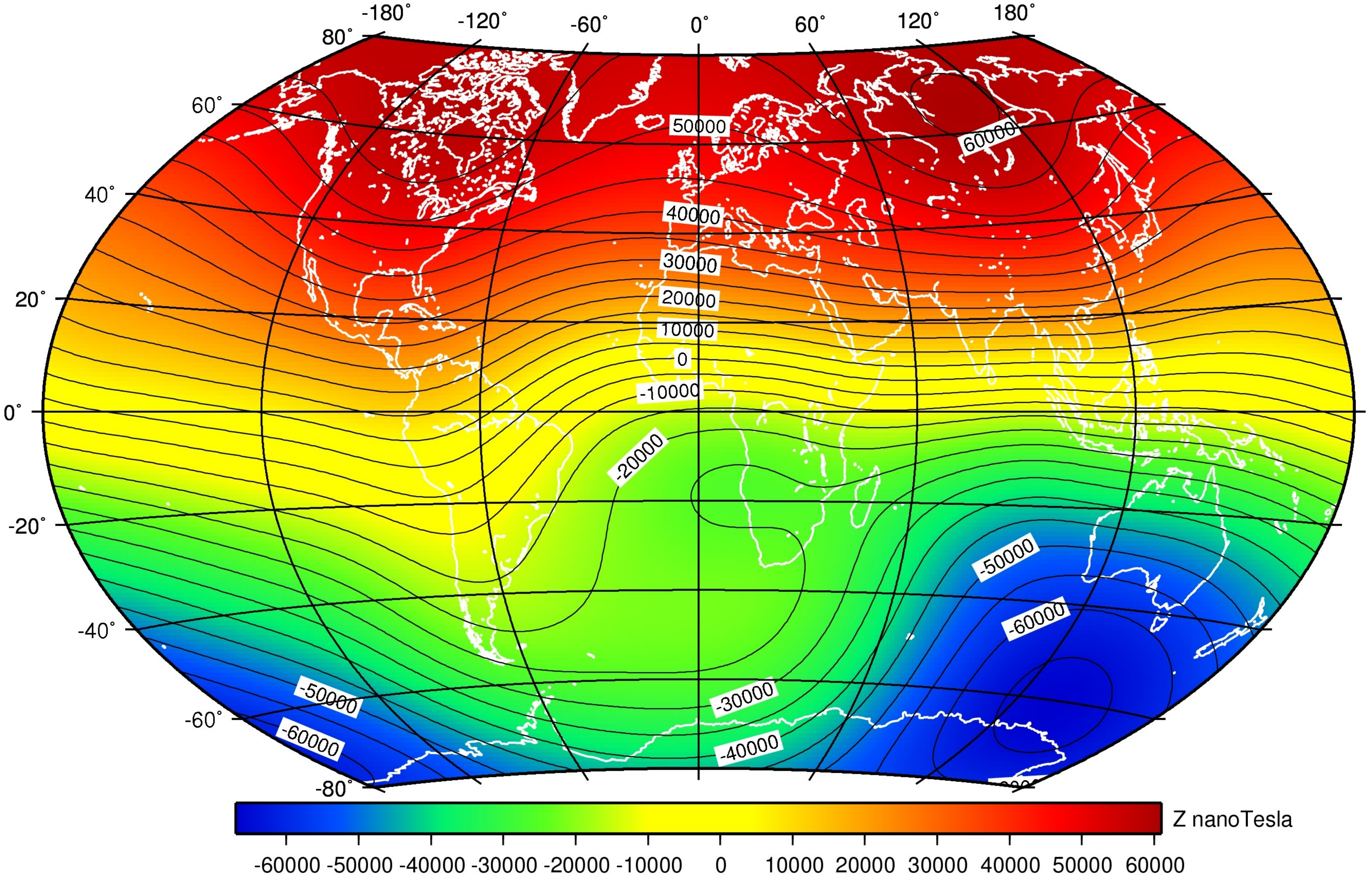

Map of predicted annual rate change of vertical intensity for 2015.0-2020.0

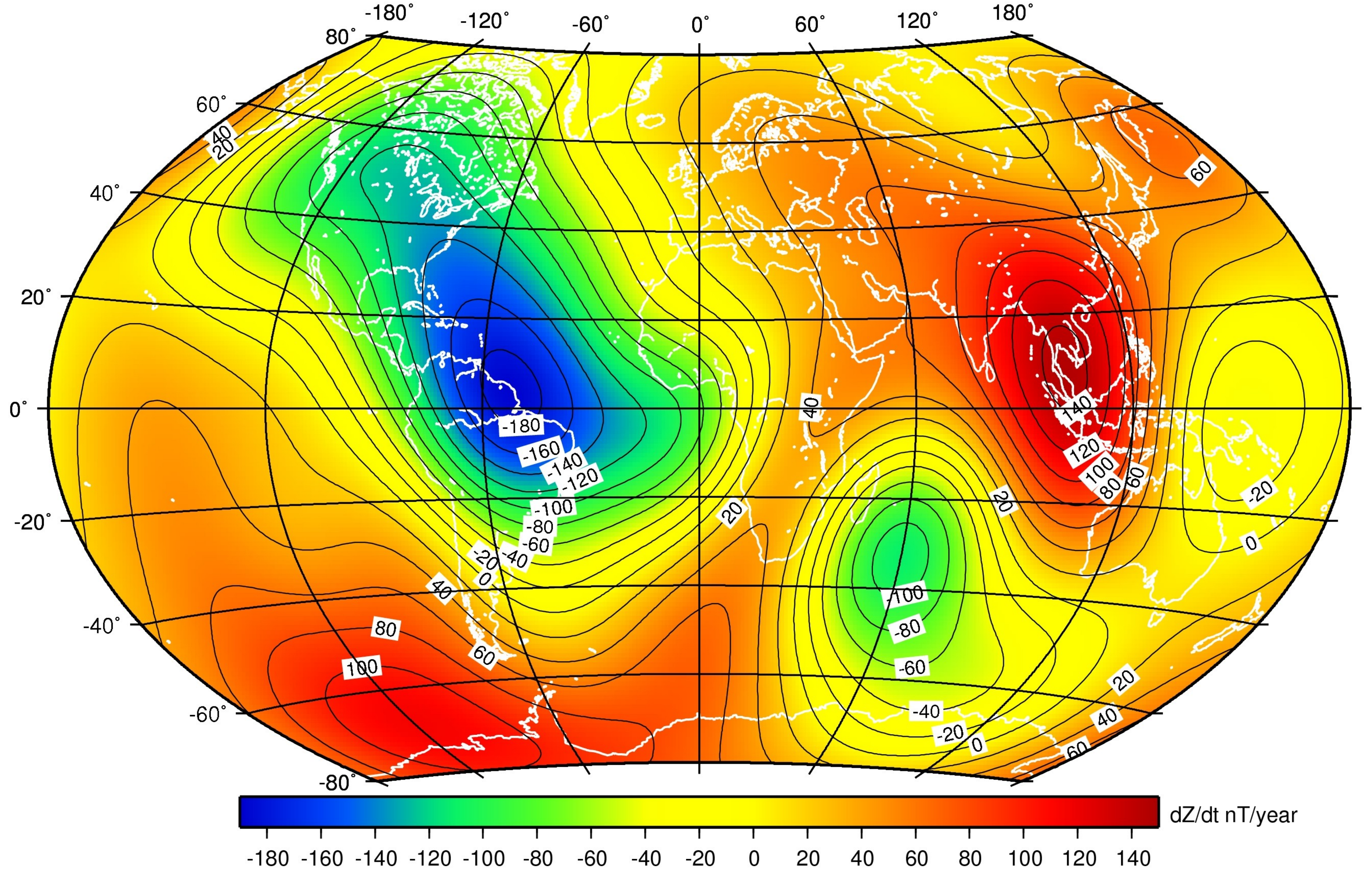

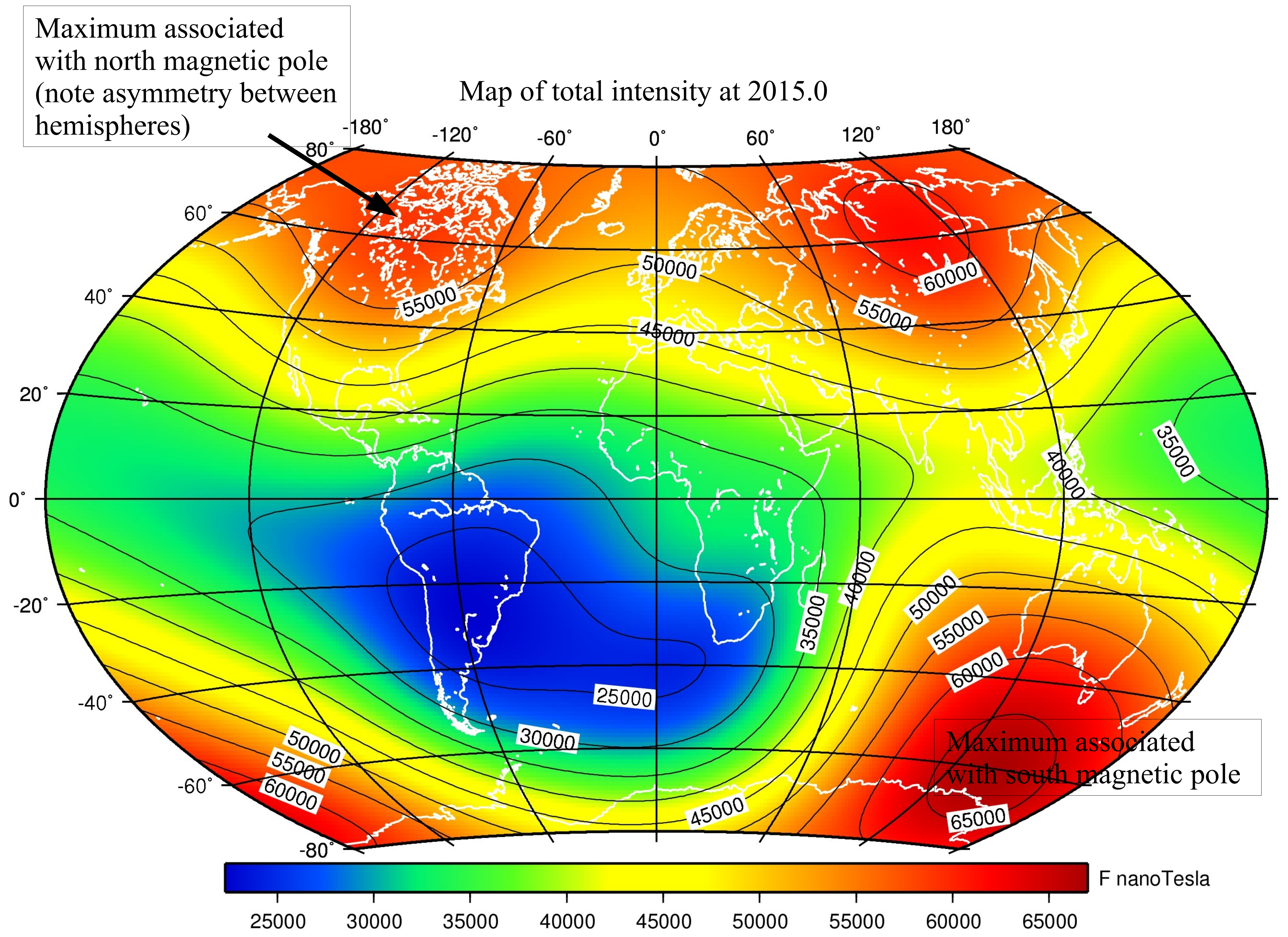
Map of total intensity at 2015.0
Maximum associated with north magnetic pole (note asymmetry between hemispheres)
Maximum associated with south magnetic pole
-180˚
-120˚
-60˚
0˚
60˚
120˚
180˚
80˚
60˚
40˚
20˚
0˚
-20˚
-40˚
-60˚
-80˚
50000
60000
55000
55000
45000
35000
40000
40000
35000
50000
55000
60000
25000
30000
50000
55000
60000
45000
65000
F nanoTesla
25000
30000
35000
40000
45000
50000
55000
60000
65000

Map of predicted annual rate of change of total intensity for 2015.0-2020.0

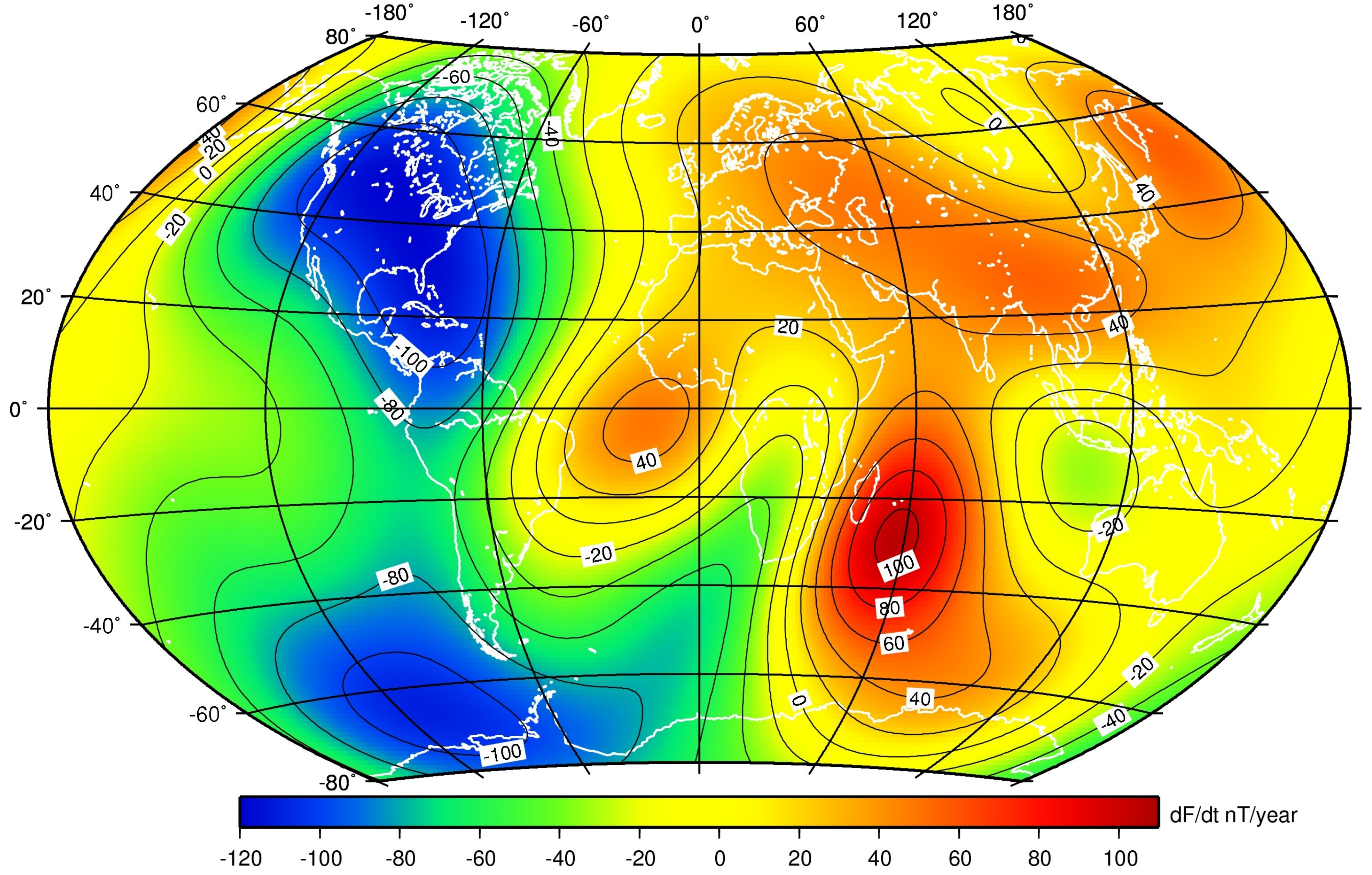

Average multipole strengths

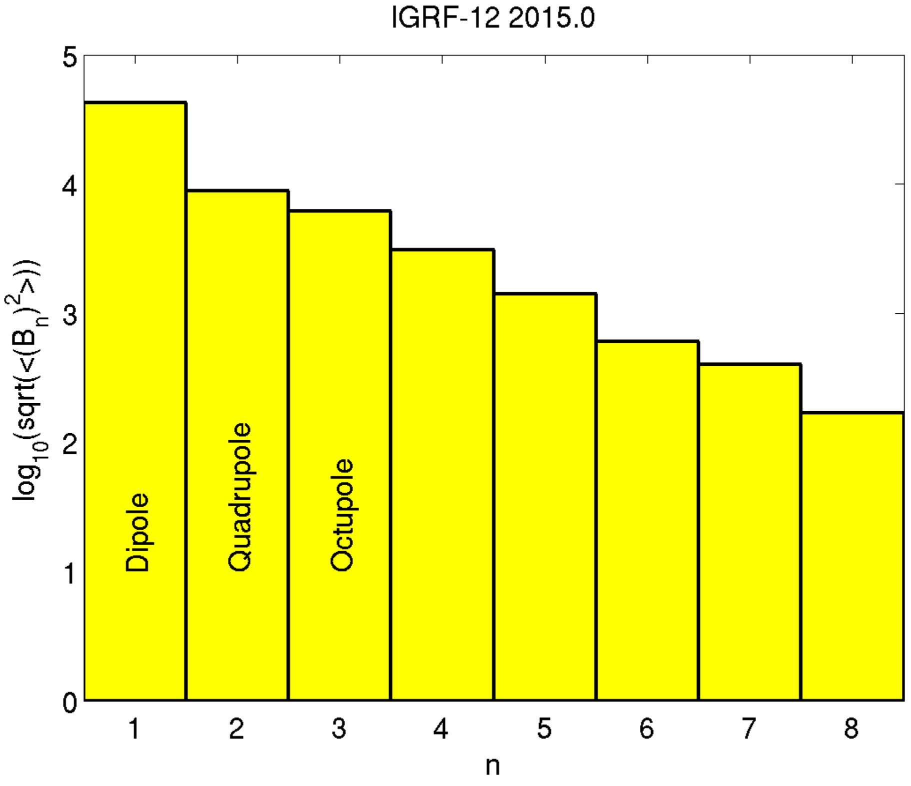

Average annual rate of change of multipole strengths

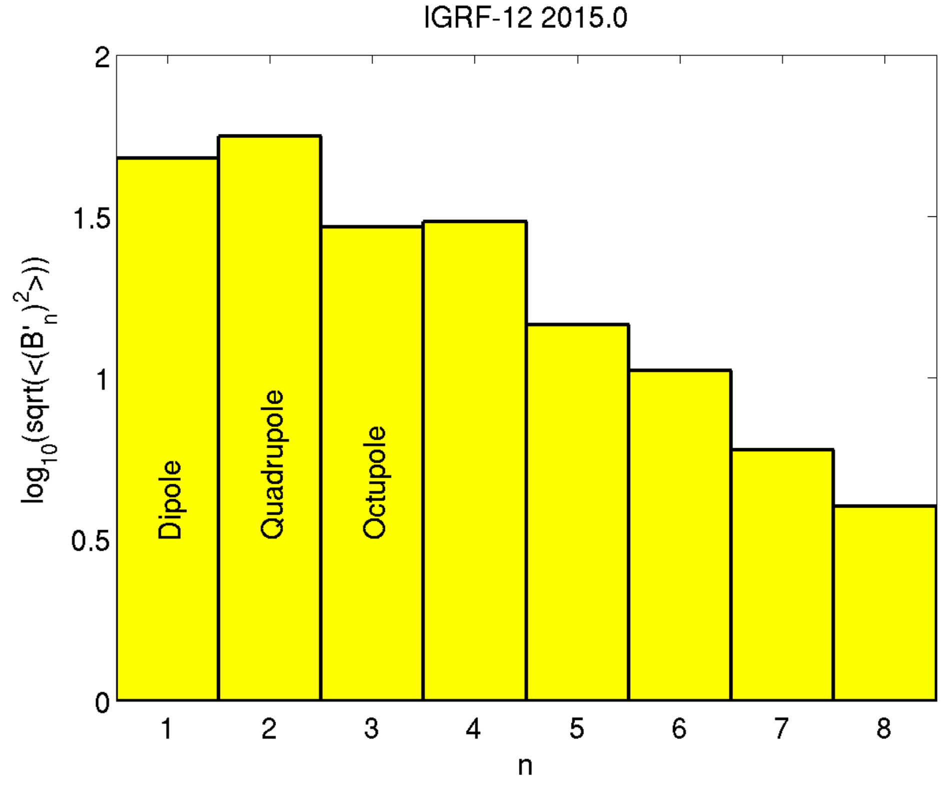

Maps of the dipole and non-dipole components of IGRF in Finland

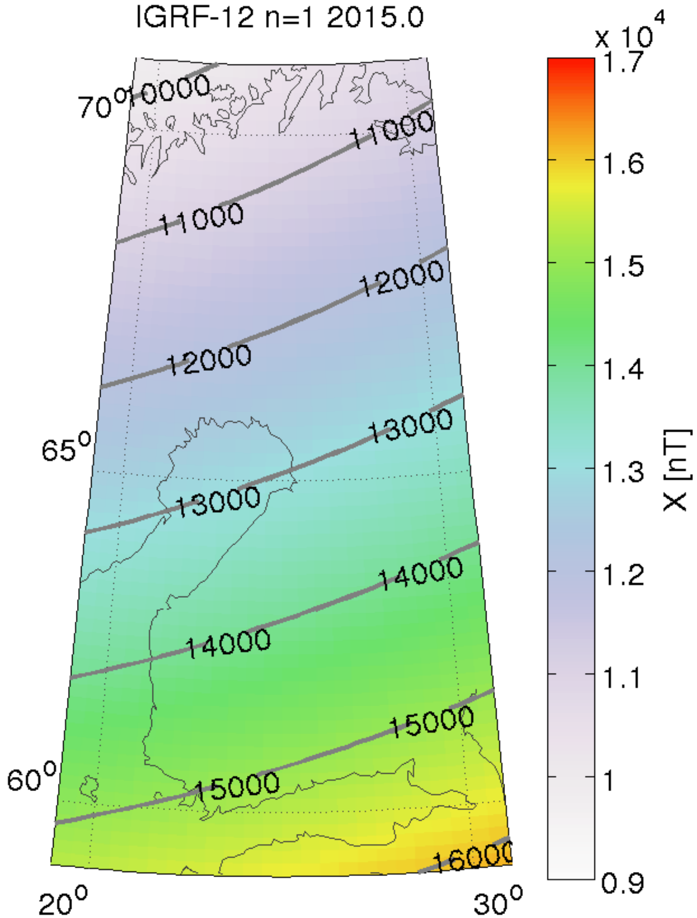
IGRF-12 n=1 2015.0
x 10^4
X [nT]
1.7
1.6
1.5
1.4
1.3
1.2
1.1
1
0.9
10000
11000
11000
12000
12000
13000
13000
14000
14000
15000
15000
16000
70°
65°
60°
20°
30°

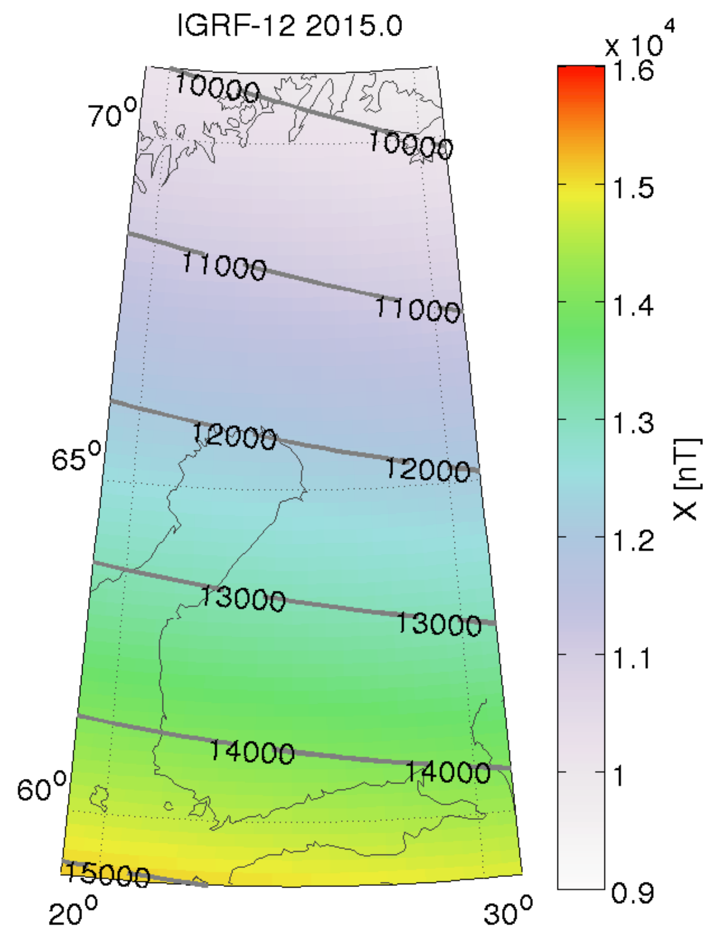
IGRF-12 2015.0
x 10^4
X [nT]
1.6
1.5
1.4
1.3
1.2
1.1
1
0.9
10000
10000
11000
11000
12000
12000
13000
13000
14000
14000
15000
70°
65°
60°
20°
30°

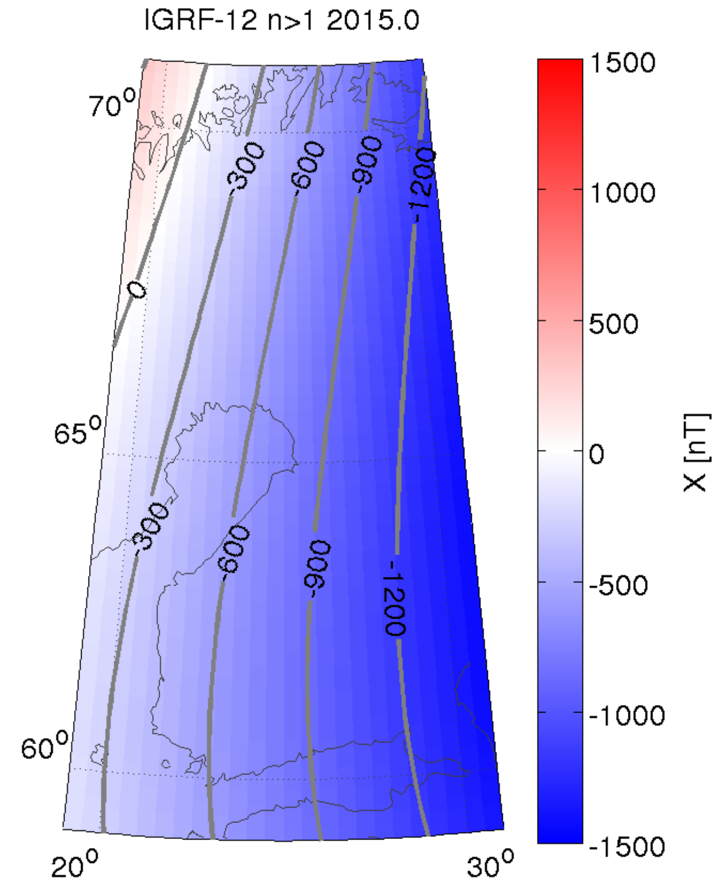
IGRF-12 n>1 2015.0
X [nT]
1500
1000
500
0
-500
-1000
-1500
0
-300
-300
-600
-600
-900
-900
-1200
-1200
70°
65°
60°
20°
30°

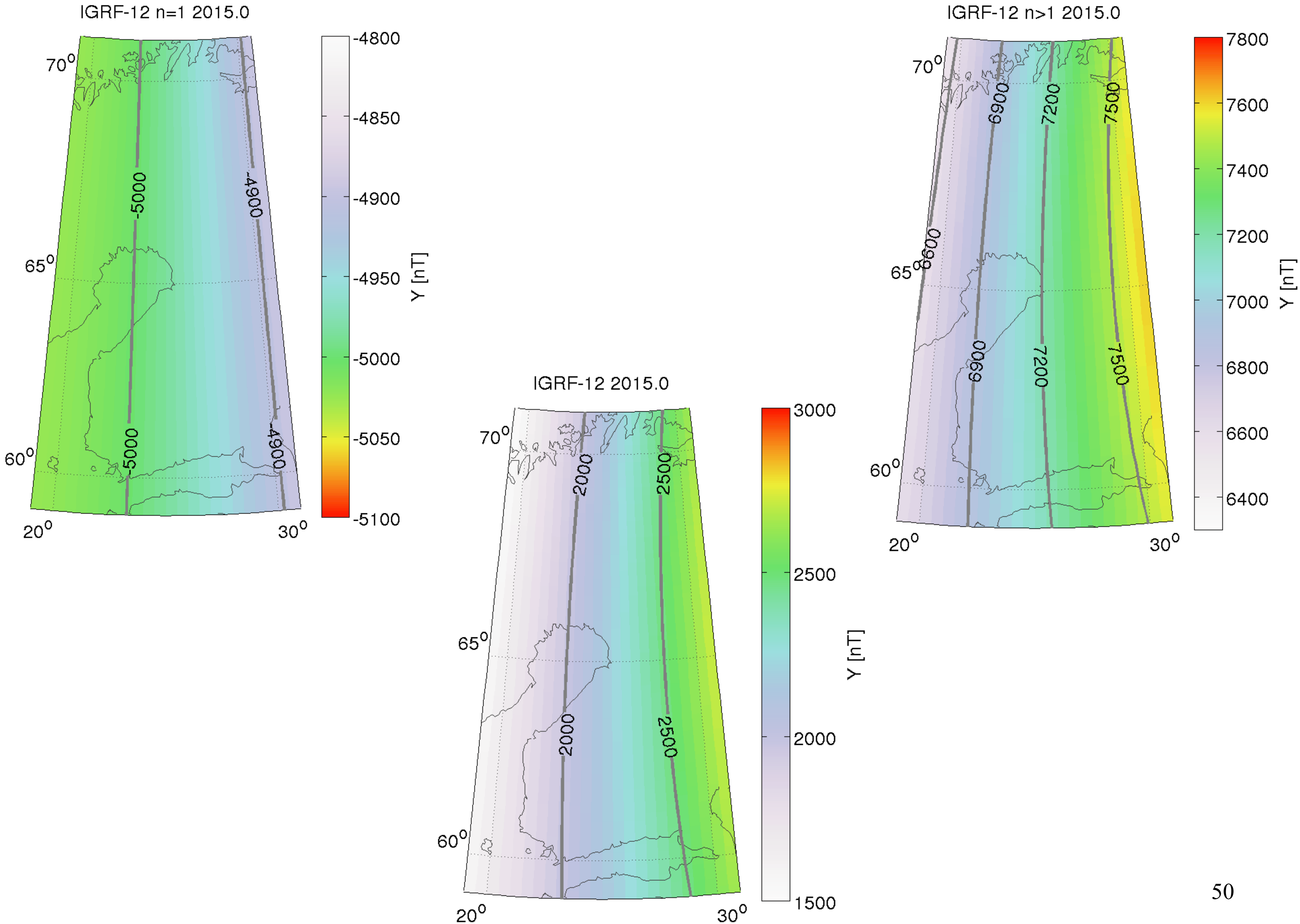
IGRF-12 n=1 2015.0
-5000
-4900
Y [nT]
-4800
-4850
-4900
-4950
-5000
-5050
-5100
IGRF-12 2015.0
2000
2500
Y [nT]
3000
2500
2000
1500
IGRF-12 n>1 2015.0
6600
6900
7200
7500
Y [nT]
7800
7600
7400
7200
7000
6800
6600
6400
70°
65°
60°
20°
30°

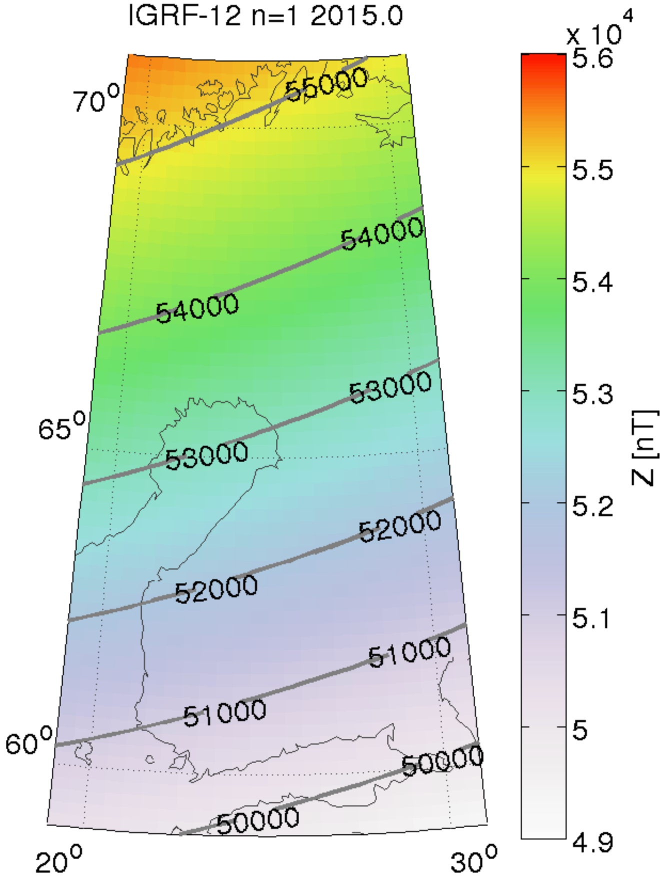
IGRF-12 n=1 2015.0
x 10^4
5.6
5.5
5.4
5.3
5.2
5.1
5
4.9
Z [nT]
55000
54000
54000
53000
53000
52000
52000
51000
51000
50000
50000
70°
65°
60°
20°
30°

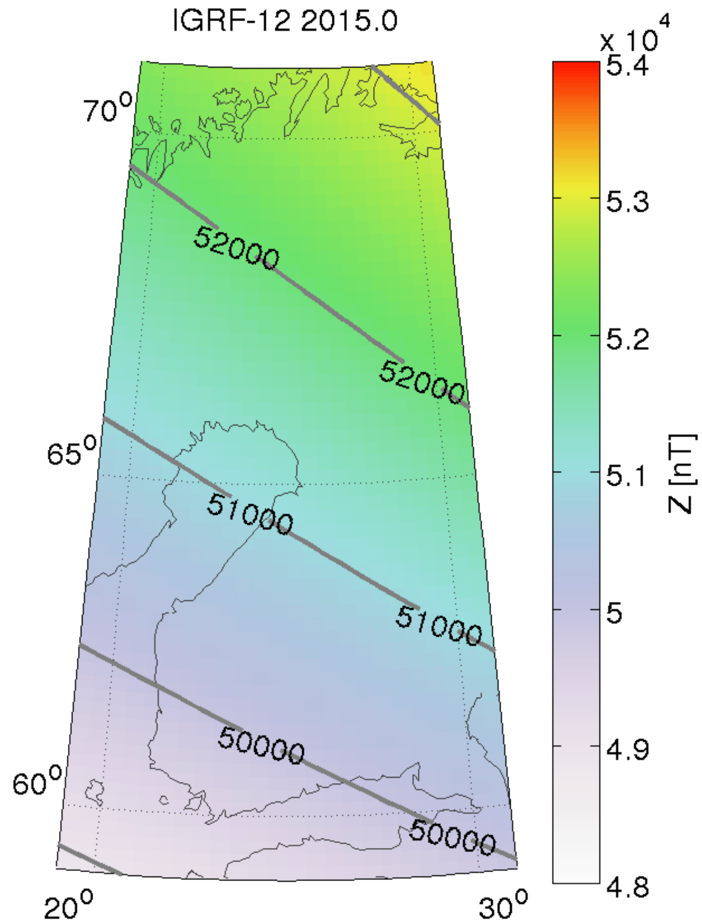
IGRF-12 2015.0
x 10^4
5.4
5.3
5.2
5.1
5
4.9
4.8
Z [nT]
52000
52000
51000
51000
50000
50000
70°
65°
60°
20°
30°

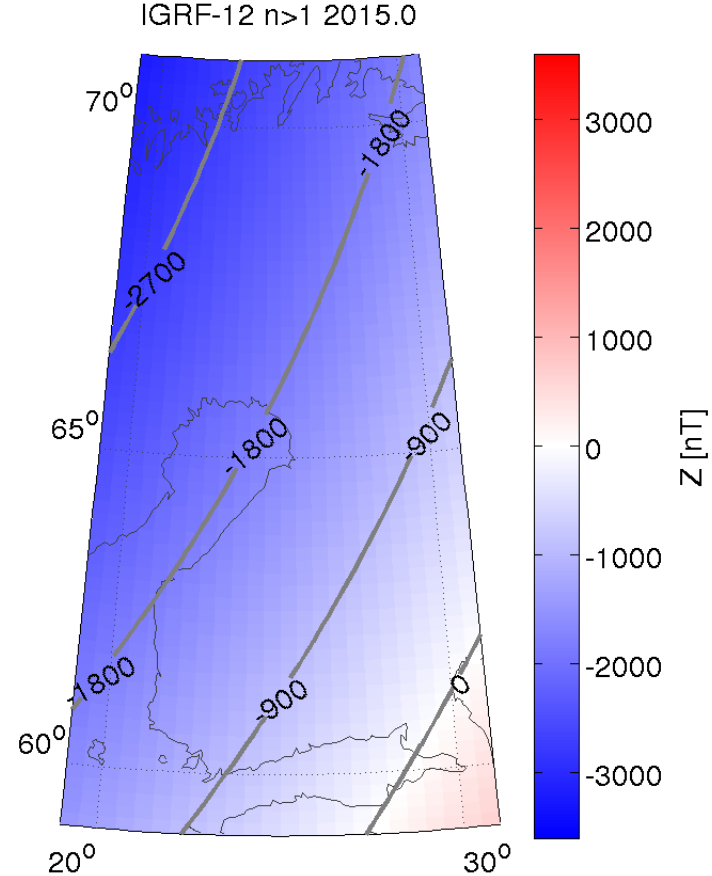
IGRF-12 n>1 2015.0
3000
2000
1000
0
-1000
-2000
-3000
Z [nT]
-2700
-1800
-1800
-1800
-900
-900
0
70°
65°
60°
20°
30°

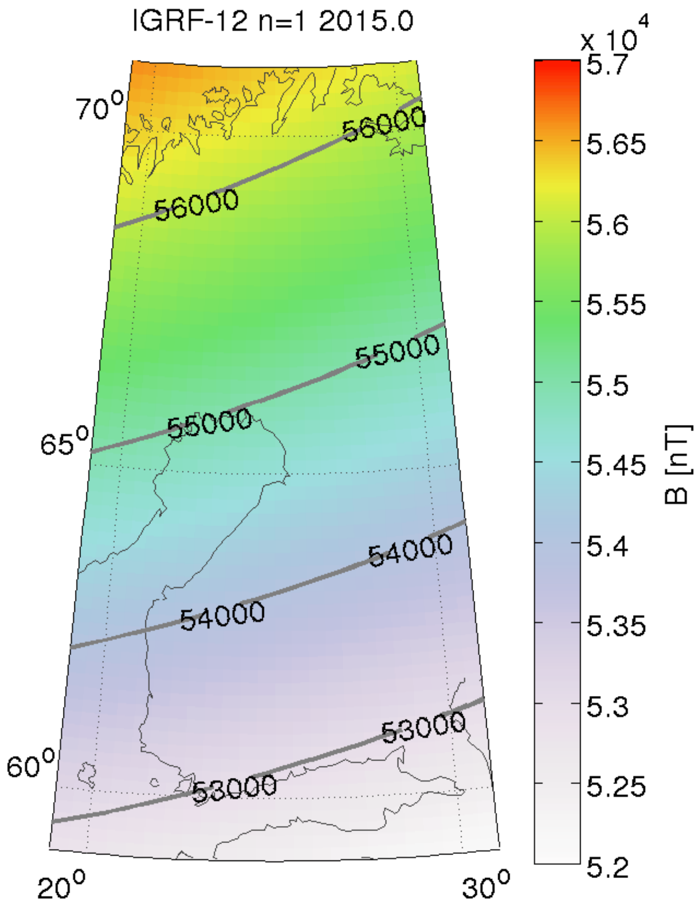
IGRF-12 n=1 2015.0
56000
55000
54000
53000
70°
65°
60°
20°
30°
x 10^4
5.7
5.65
5.6
5.55
5.5
5.45
5.4
5.35
5.3
5.25
5.2
B [nT]

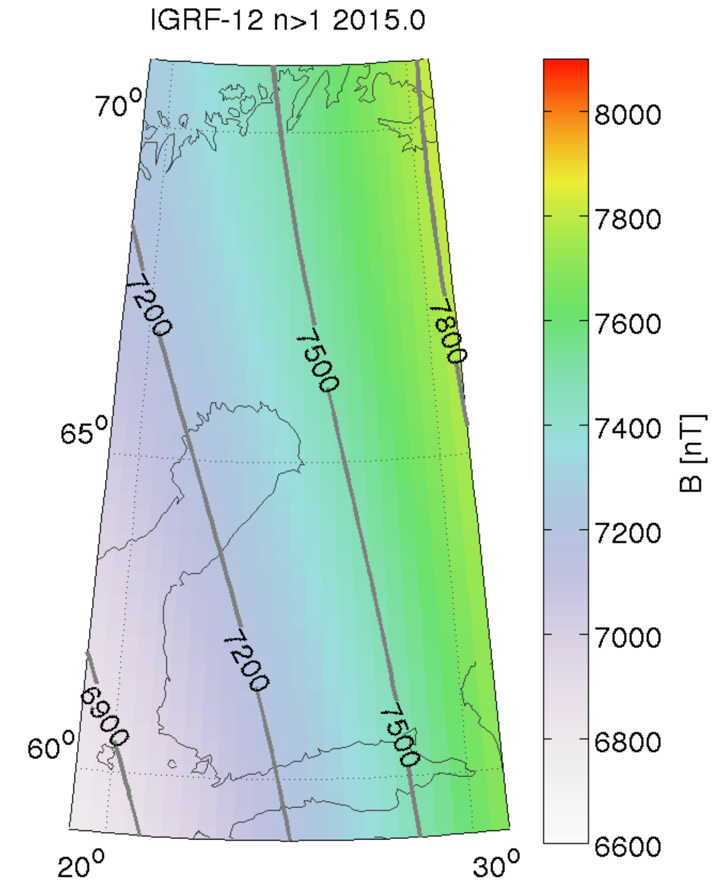
IGRF-12 n>1 2015.0
7200
7500
7800
6900
70°
65°
60°
20°
30°
8000
7800
7600
7400
7200
7000
6800
6600
B [nT]

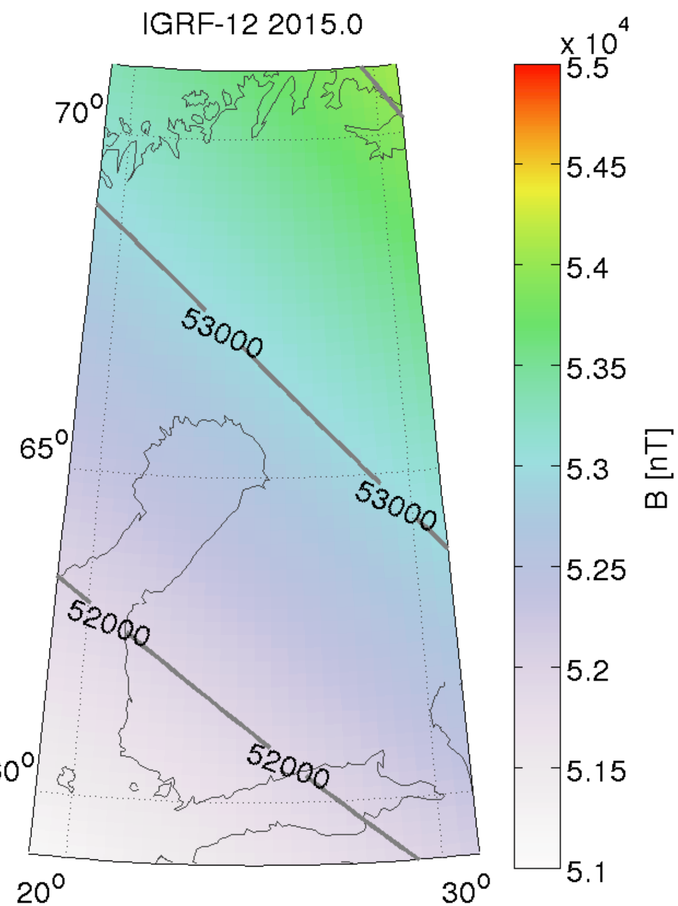
IGRF-12 2015.0
53000
52000
70°
65°
60°
20°
30°
x 10^4
5.5
5.45
5.4
5.35
5.3
5.25
5.2
5.15
5.1
B [nT]

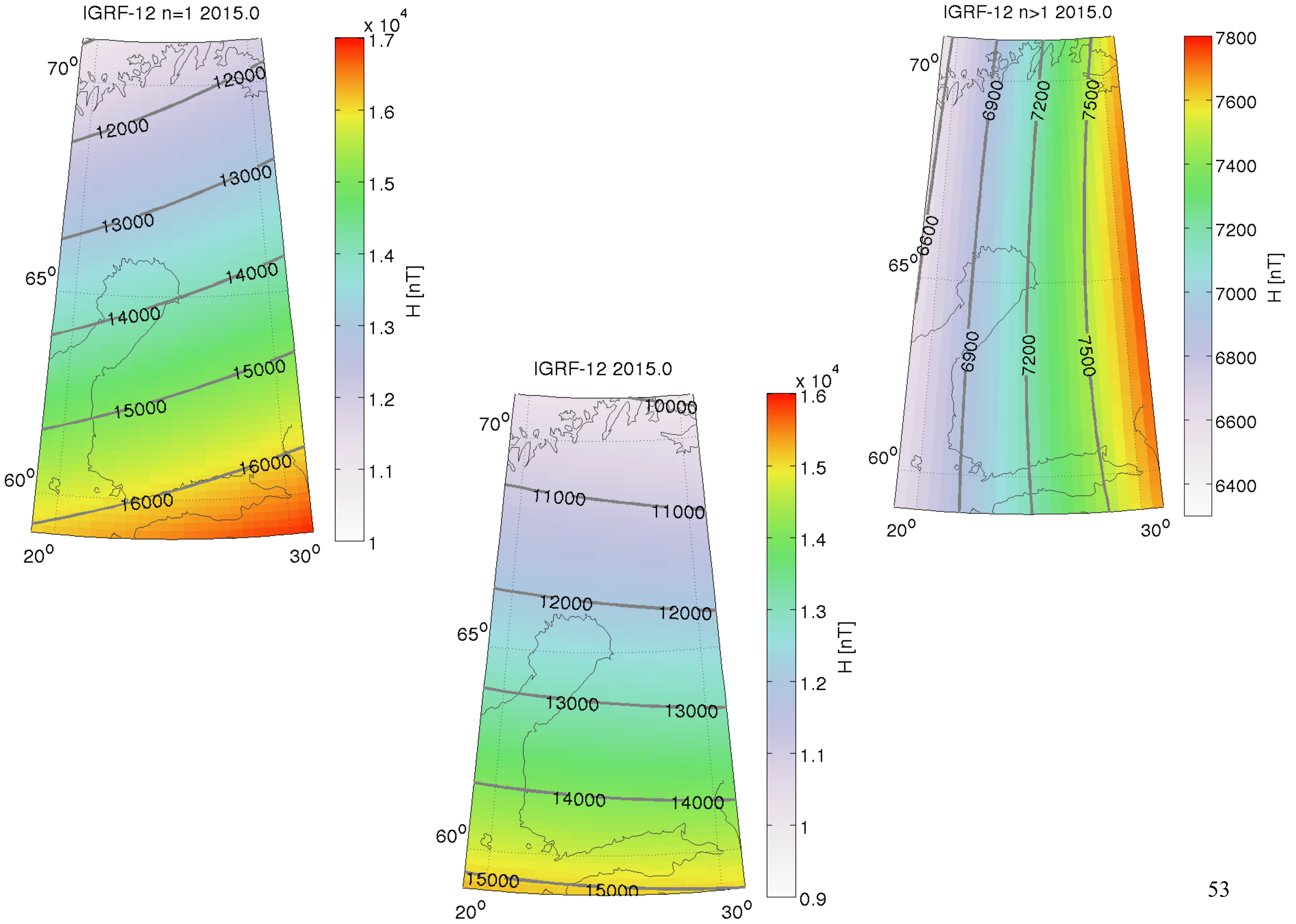
IGRF-12 n=1 2015.0
x 10^4
H [nT]
12000
13000
14000
15000
16000
70°
65°
60°
20°
30°
IGRF-12 2015.0
10000
11000
12000
13000
14000
15000
IGRF-12 n>1 2015.0
6600
6900
7200
7500

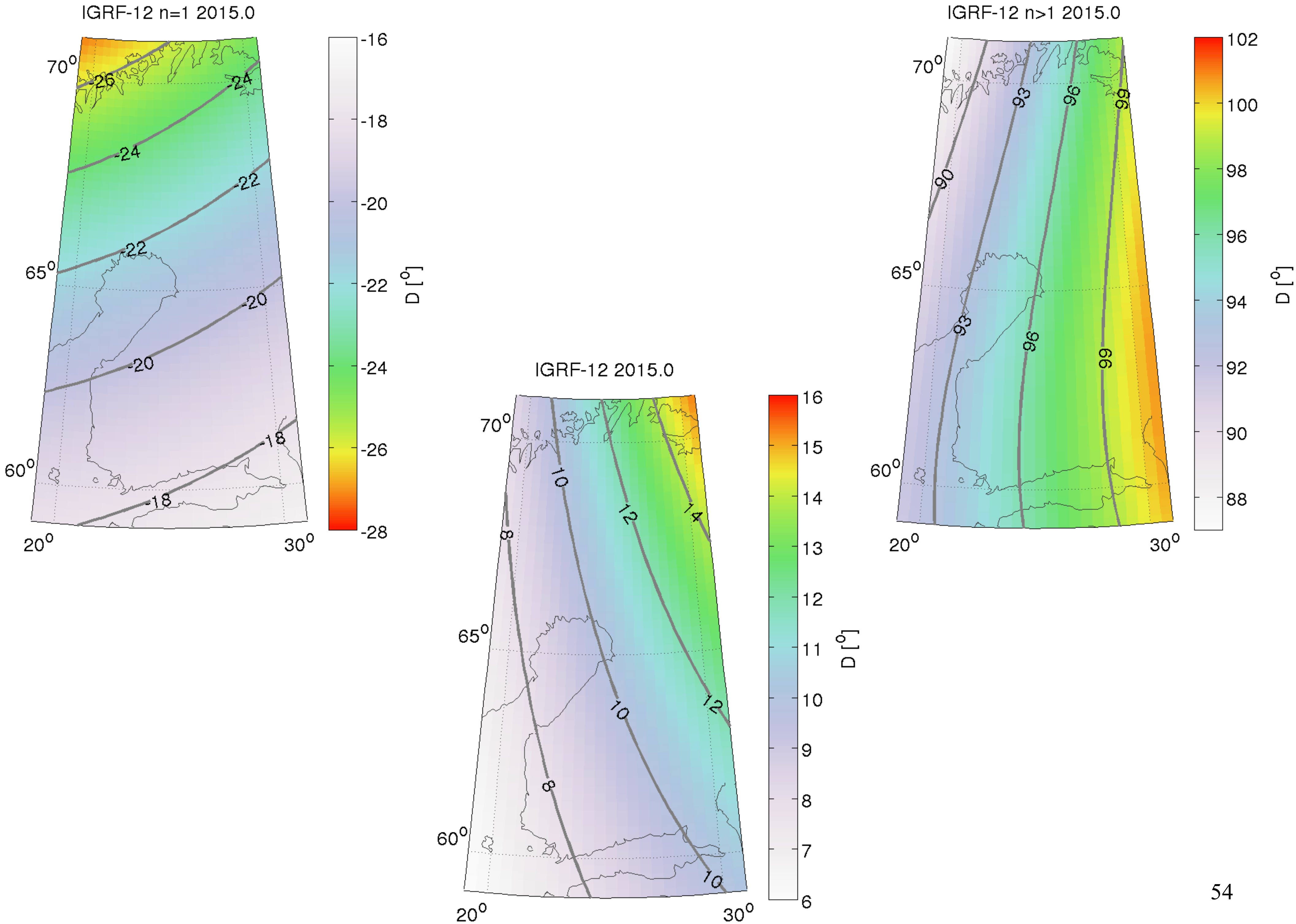

IGRF-12 n=1 2015.0
70°
65°
60°
20°
30°
-26
-24
-24
-22
-22
-20
-20
-18
-18
-16
-18
-20
-22
-24
-26
-28
D [°]
IGRF-12 2015.0
70°
65°
60°
20°
30°
8
8
10
10
10
12
12
14
16
15
14
13
12
11
10
9
8
7
6
D [°]
IGRF-12 n>1 2015.0
70°
65°
60°
20°
30°
90
93
93
96
96
99
99
102
100
98
96
94
92
90
88
D [°]

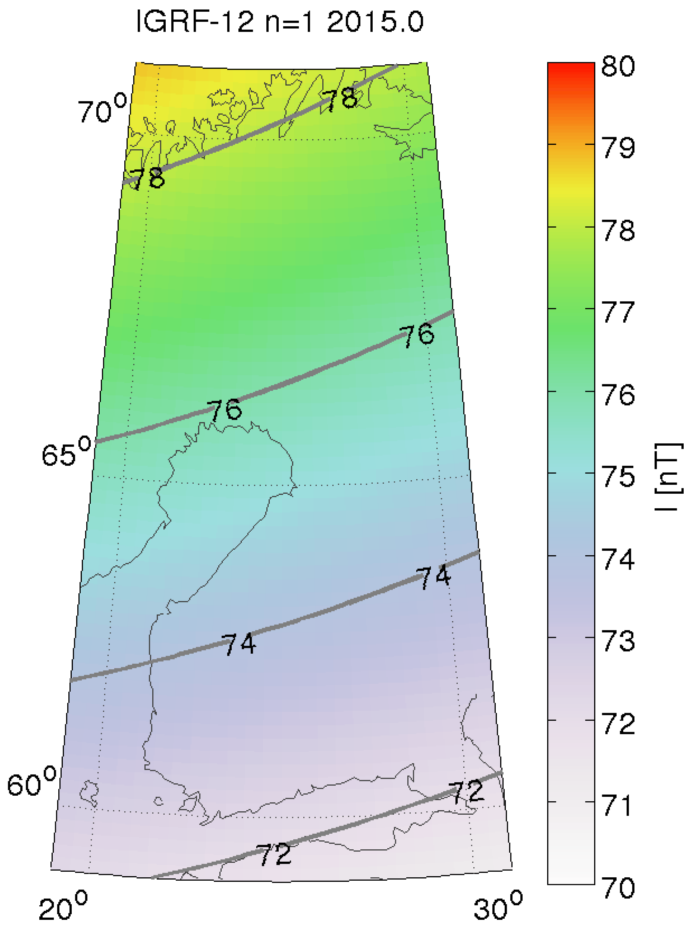
IGRF-12 n=1 2015.0
I [nT]

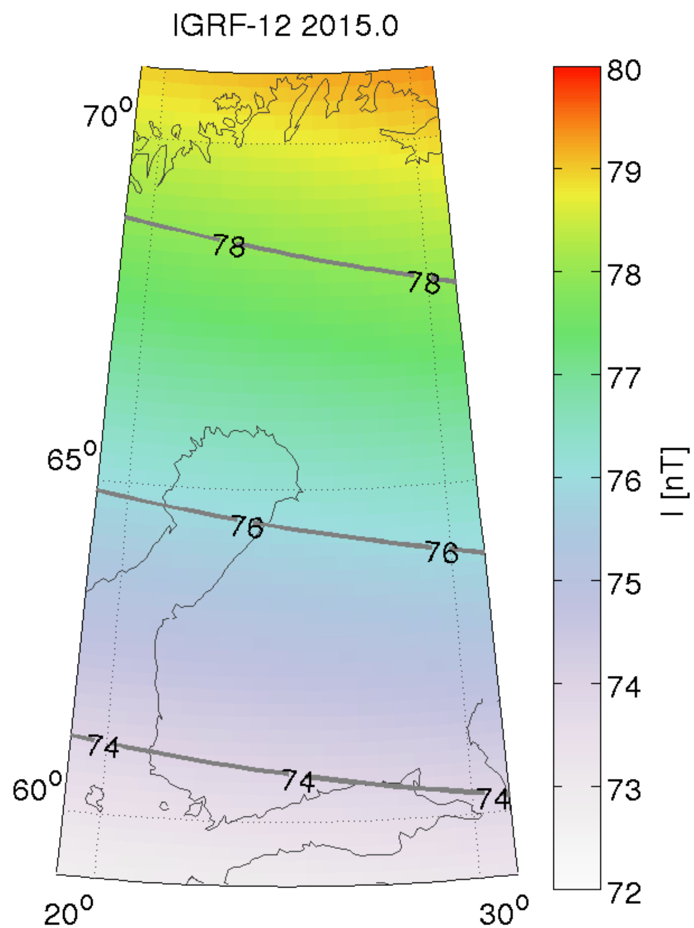
IGRF-12 2015.0
I [nT]

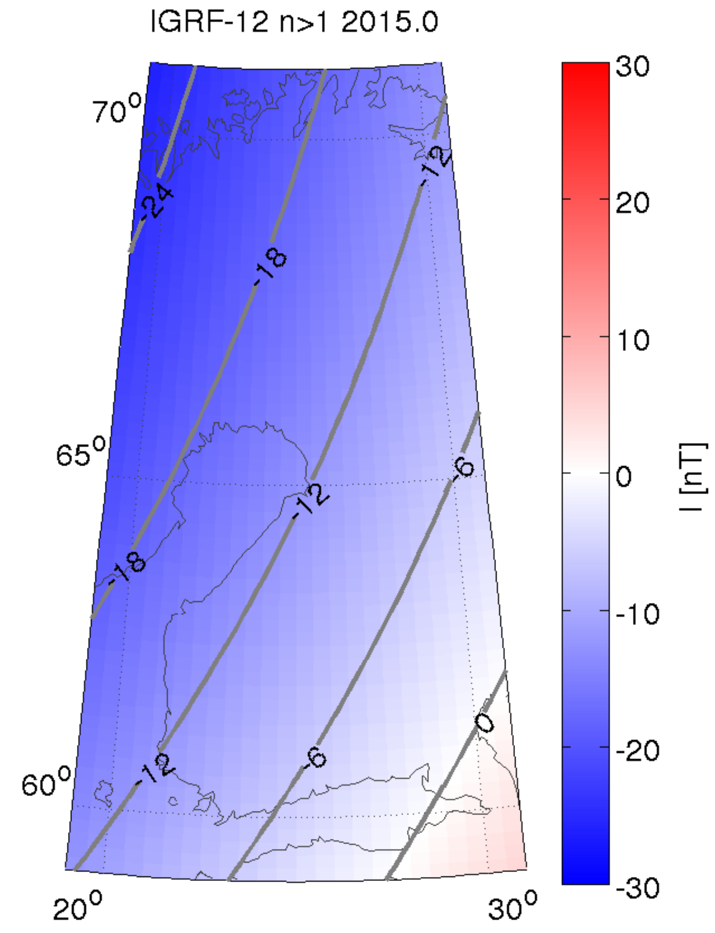
IGRF-12 n>1 2015.0
I [nT]

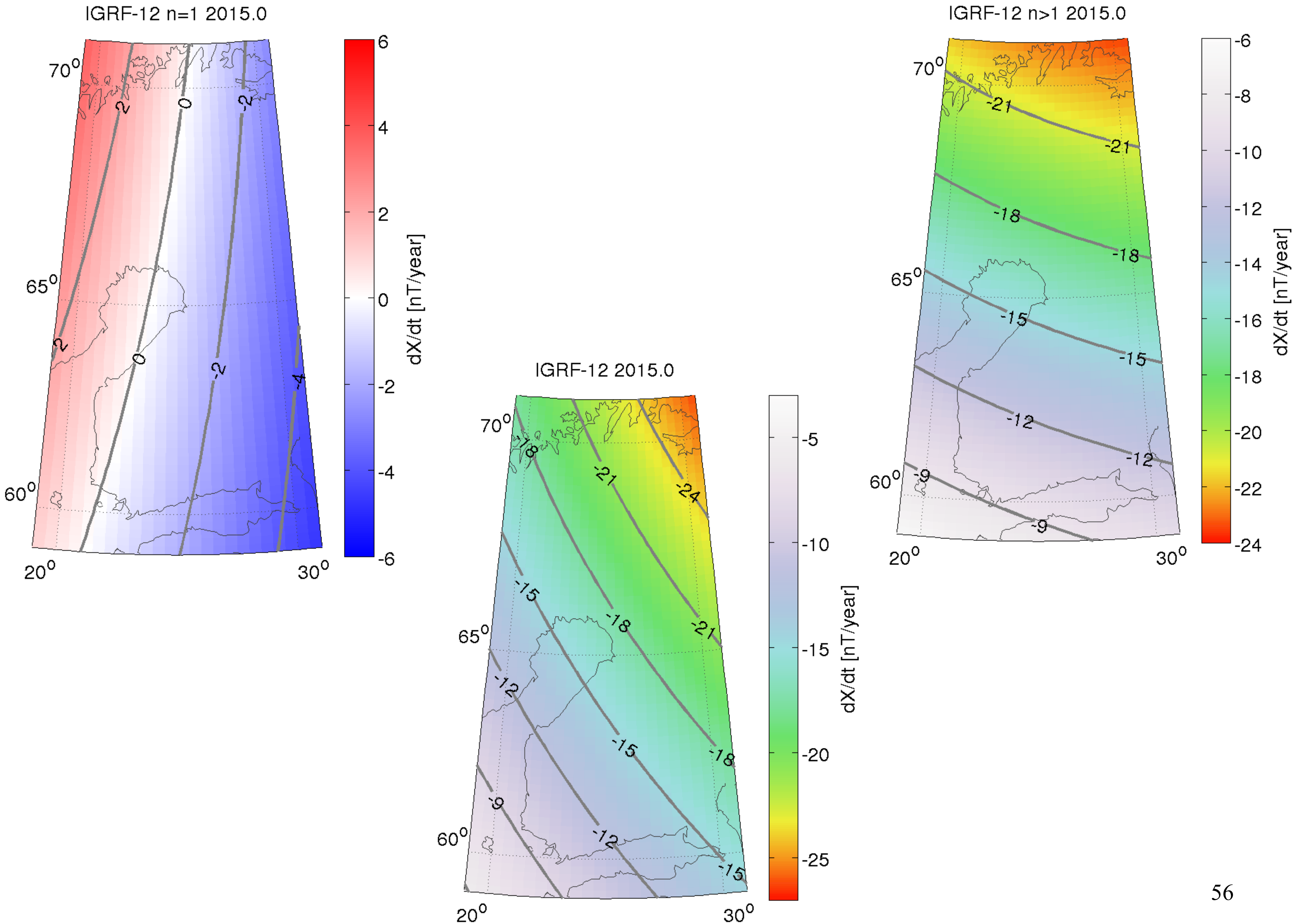
IGRF-12 n=1 2015.0
IGRF-12 2015.0
IGRF-12 n>1 2015.0
dX/dt [nT/year]
dX/dt [nT/year]
dX/dt [nT/year]
70^0
65^0
60^0
20^0
30^0

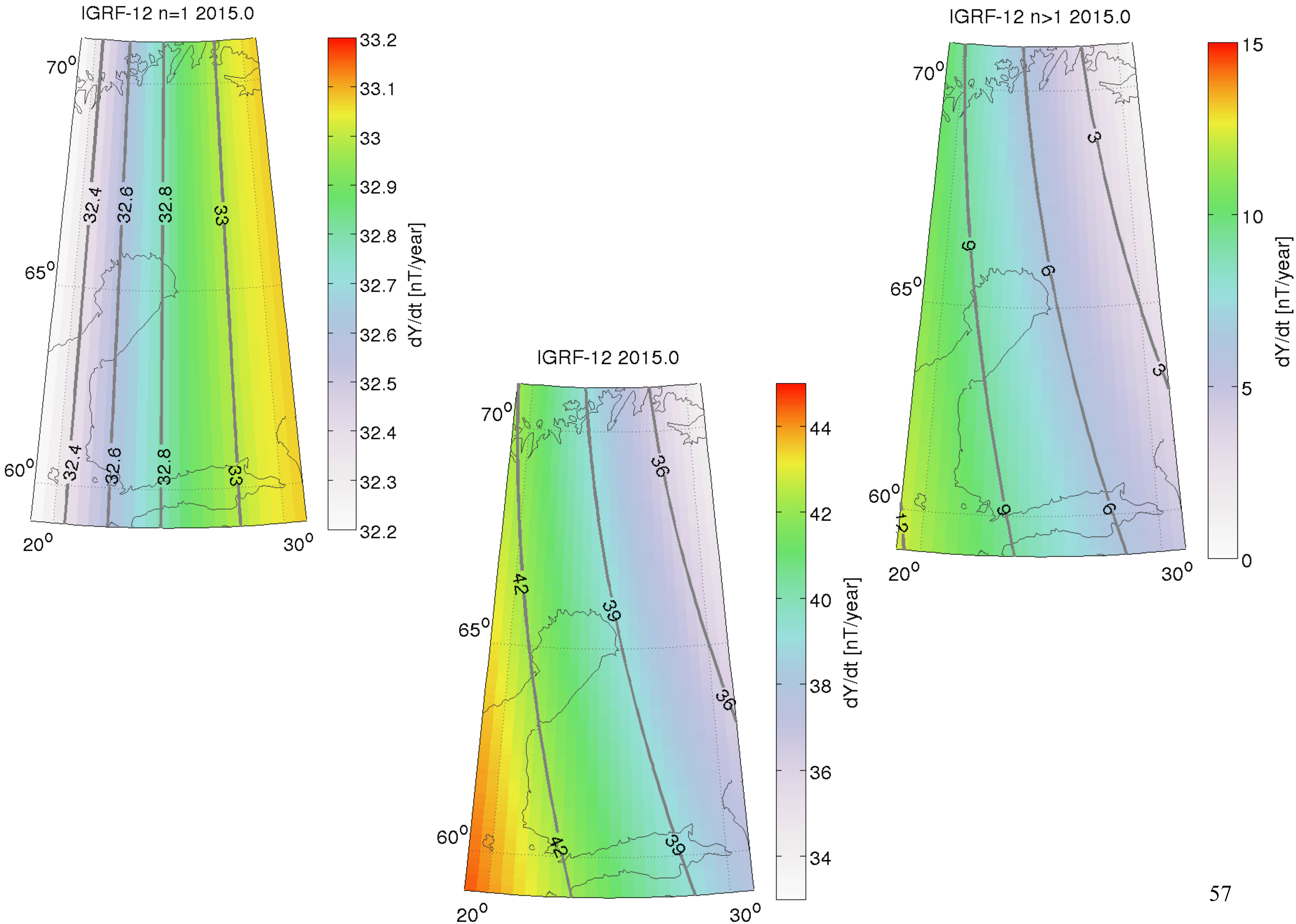
IGRF-12 n=1 2015.0
dY/dt [nT/year]
IGRF-12 2015.0
dY/dt [nT/year]
IGRF-12 n>1 2015.0
dY/dt [nT/year]

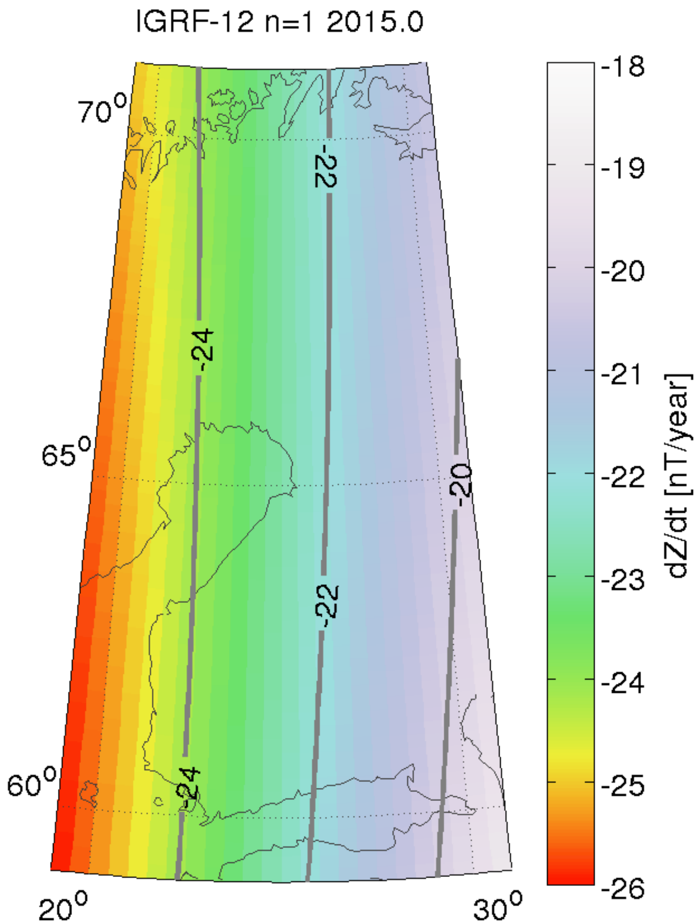

IGRF-12 n=1 2015.0
70°
65°
60°
20°
30°
-24
-22
-20
-18
-19
-20
-21
-22
-23
-24
-25
-26
dZ/dt [nT/year]

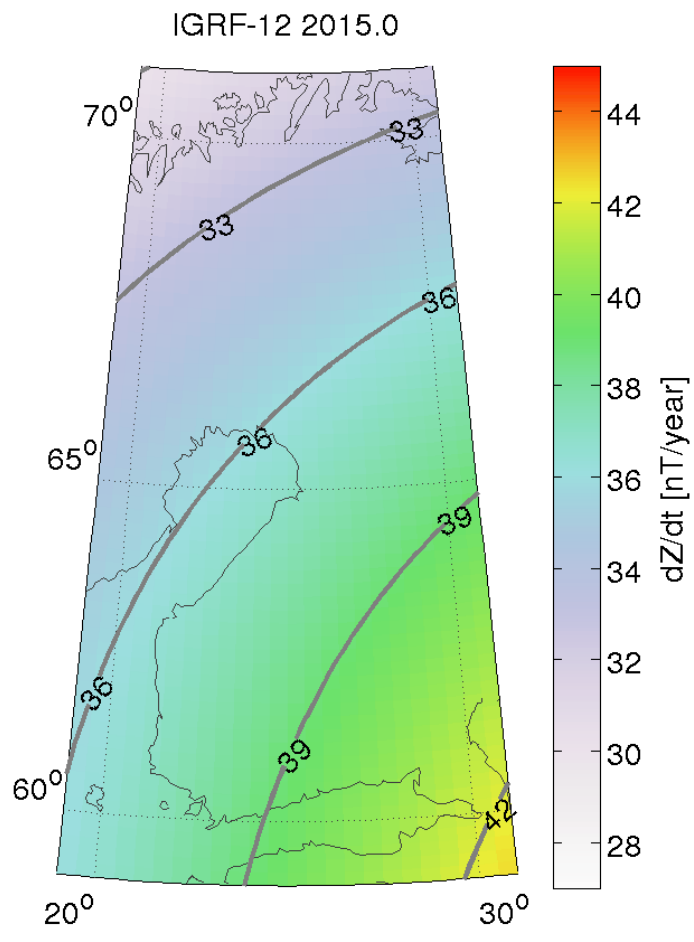

IGRF-12 2015.0
70°
65°
60°
20°
30°
33
36
39
42
44
42
40
38
36
34
32
30
28
dZ/dt [nT/year]

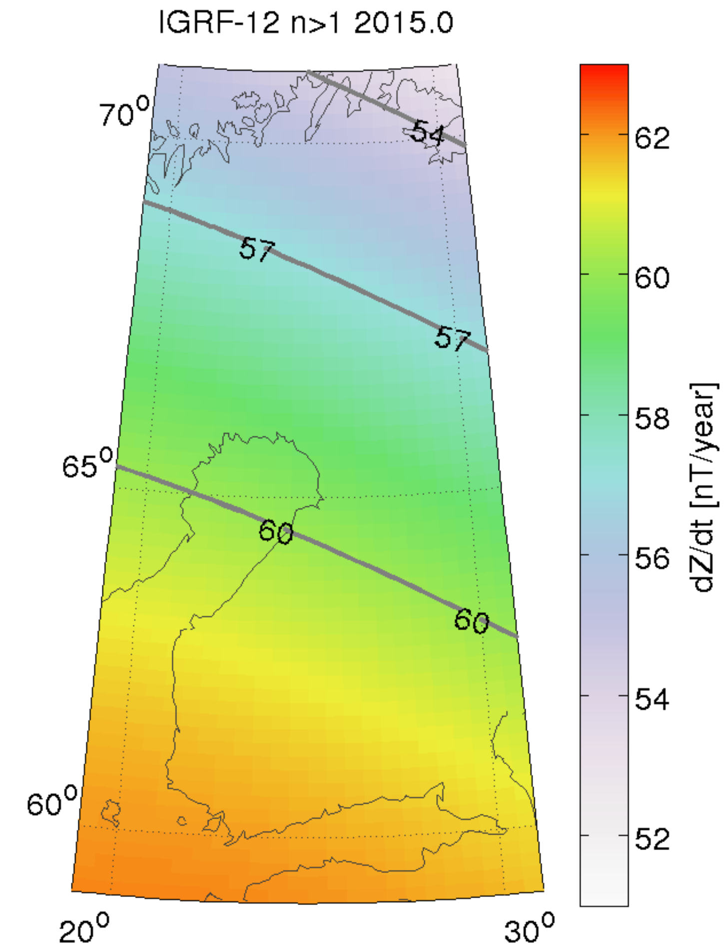

IGRF-12 n>1 2015.0
70°
65°
60°
20°
30°
54
57
60
62
60
58
56
54
52
dZ/dt [nT/year]

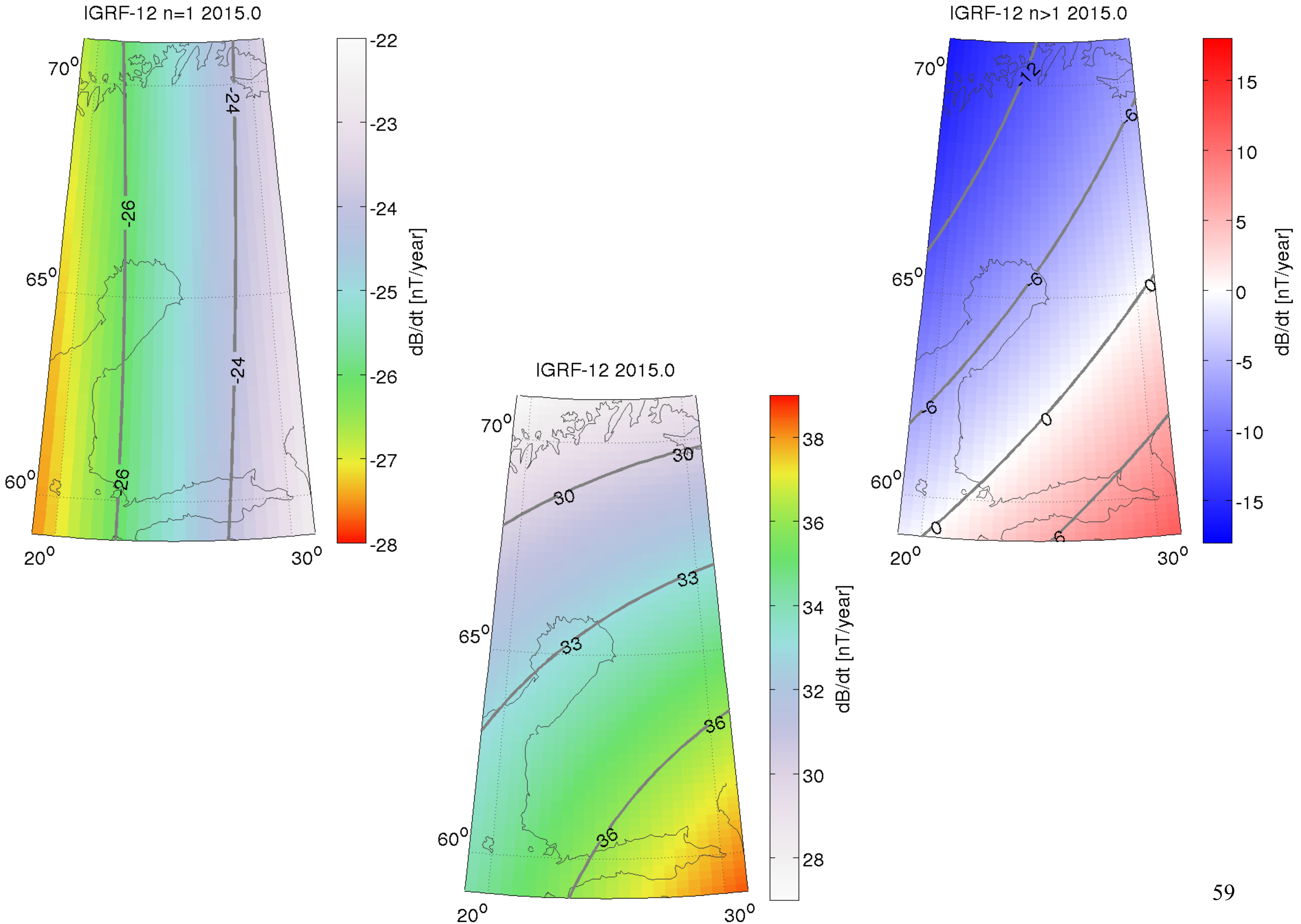
IGRF-12 n=1 2015.0
dB/dt [nT/year]
IGRF-12 2015.0
dB/dt [nT/year]
IGRF-12 n>1 2015.0
dB/dt [nT/year]

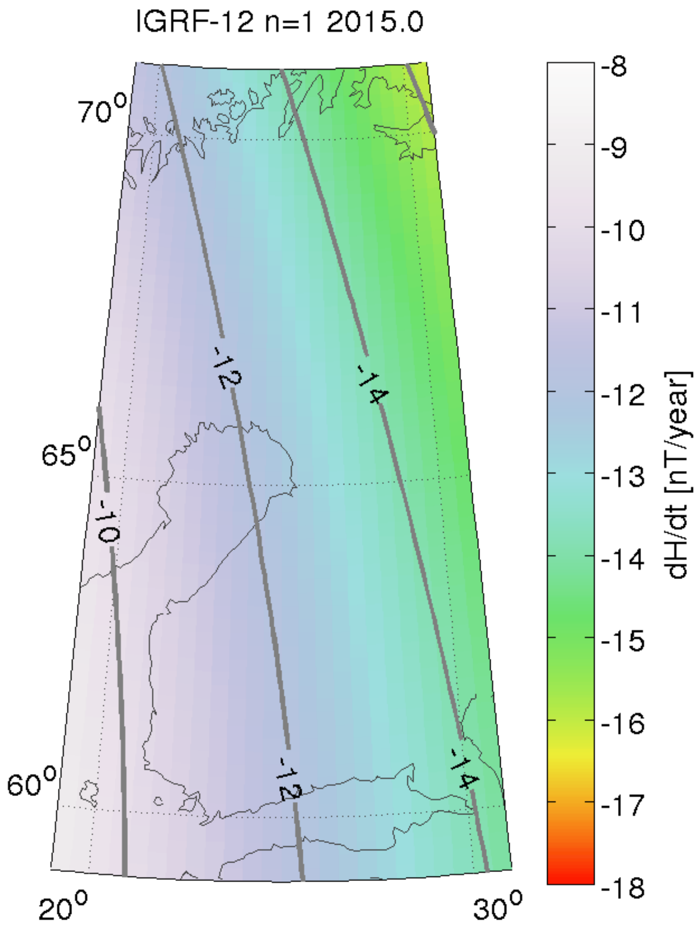
IGRF-12 n=1 2015.0
70°
65°
60°
20°
30°
-12
-14
-10
-8
-9
-10
-11
-12
-13
-14
-15
-16
-17
-18
dH/dt [nT/year]

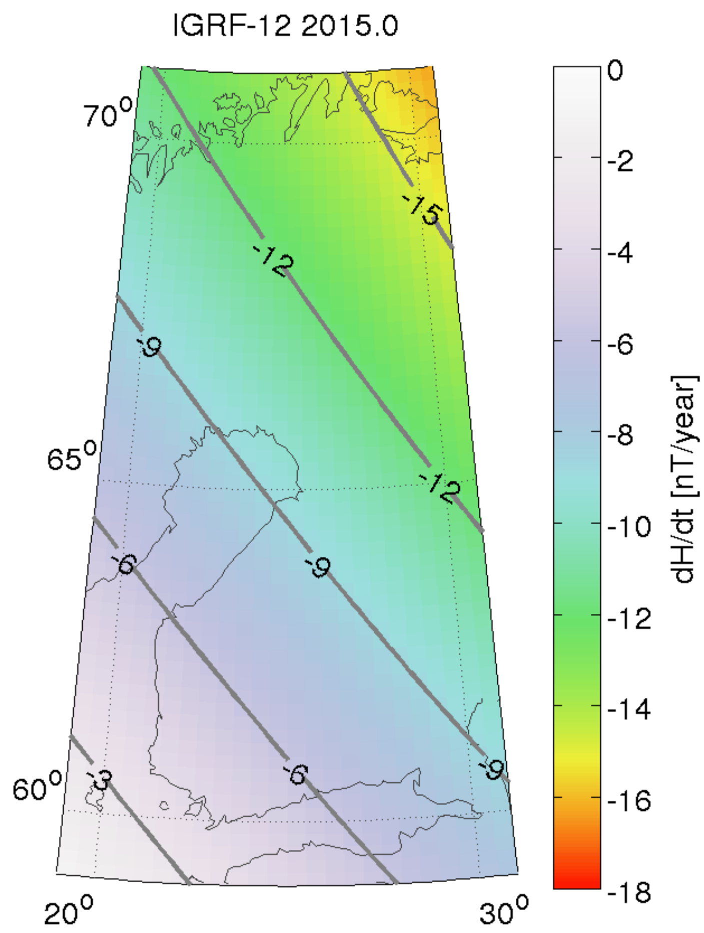
IGRF-12 2015.0
70°
65°
60°
20°
30°
-15
-12
-9
-6
-3
0
-2
-4
-6
-8
-10
-12
-14
-16
-18
dH/dt [nT/year]

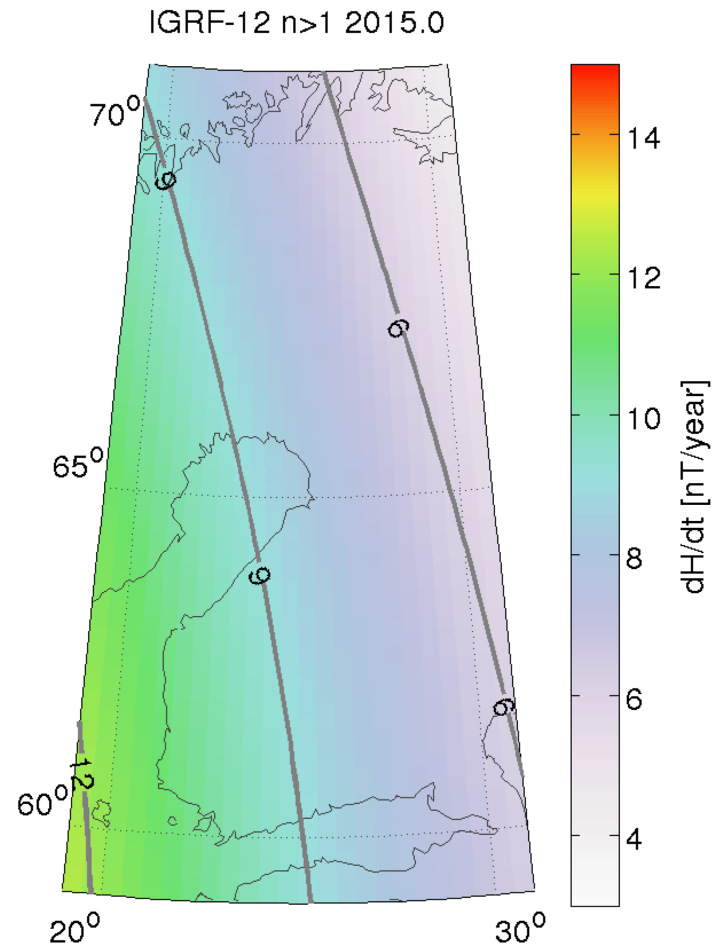
IGRF-12 n>1 2015.0
70°
65°
60°
20°
30°
9
6
12
14
12
10
8
6
4
dH/dt [nT/year]

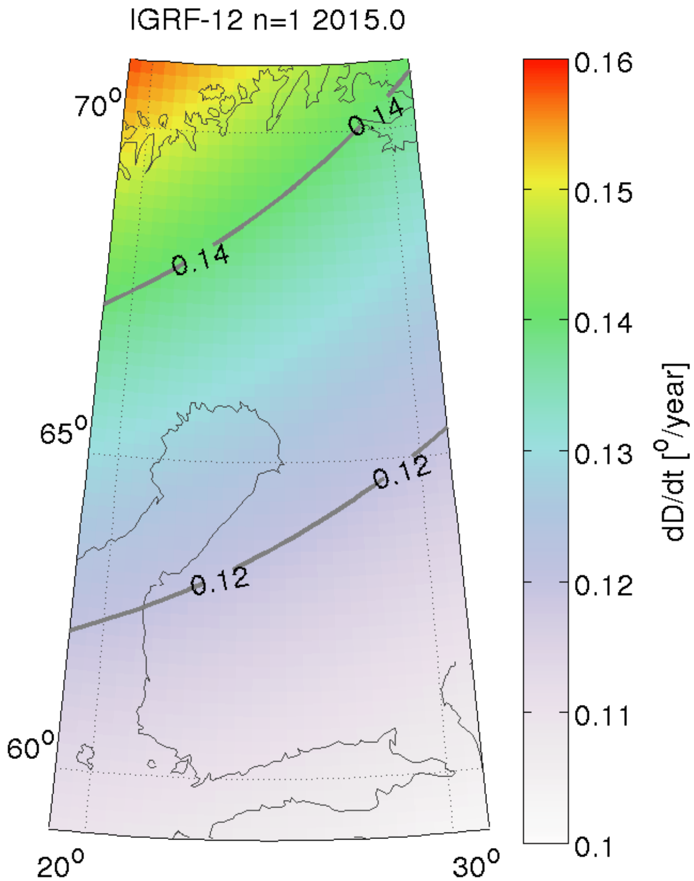
IGRF-12 n=1 2015.0
70°
65°
60°
20°
30°
0.14
0.14
0.12
0.12
0.16
0.15
0.14
0.13
0.12
0.11
0.1
dD/dt [°/year]

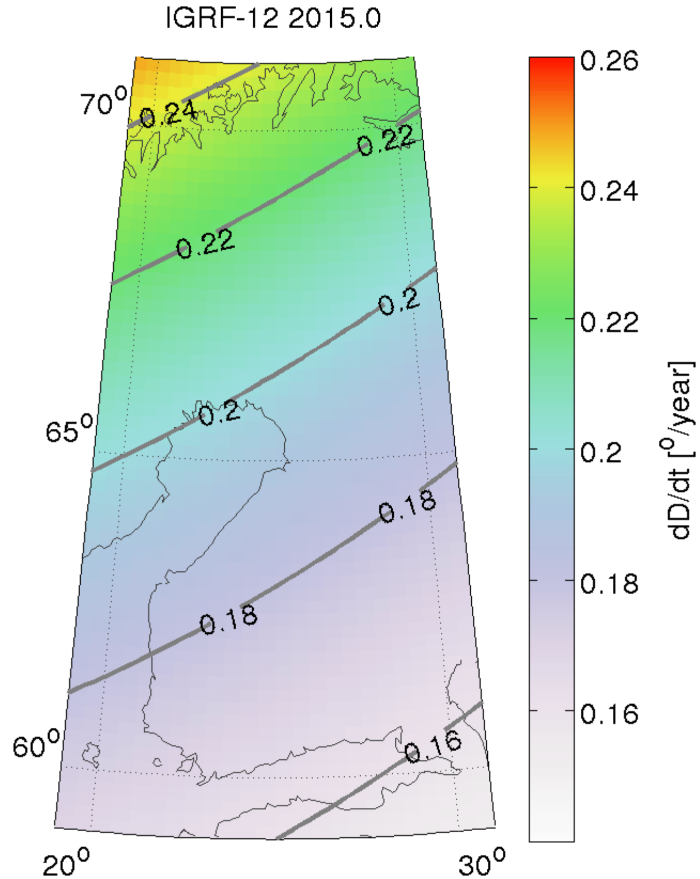
IGRF-12 2015.0
70°
65°
60°
20°
30°
0.24
0.22
0.22
0.2
0.2
0.18
0.18
0.16
0.26
0.24
0.22
0.2
0.18
0.16
dD/dt [°/year]

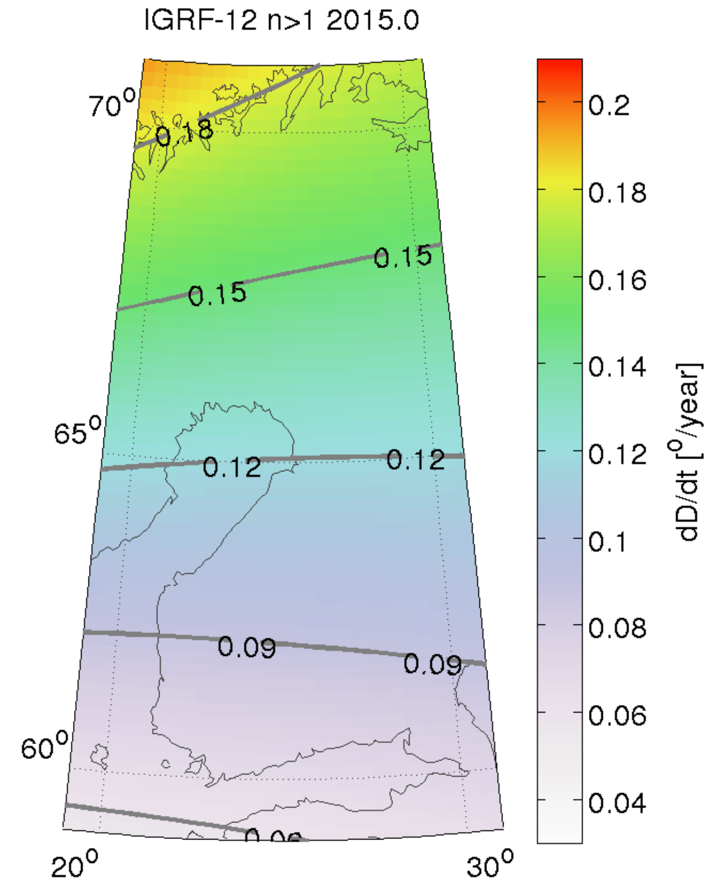
IGRF-12 n>1 2015.0
70°
65°
60°
20°
30°
0.18
0.15
0.15
0.12
0.12
0.09
0.09
0.2
0.18
0.16
0.14
0.12
0.1
0.08
0.06
0.04
dD/dt [°/year]

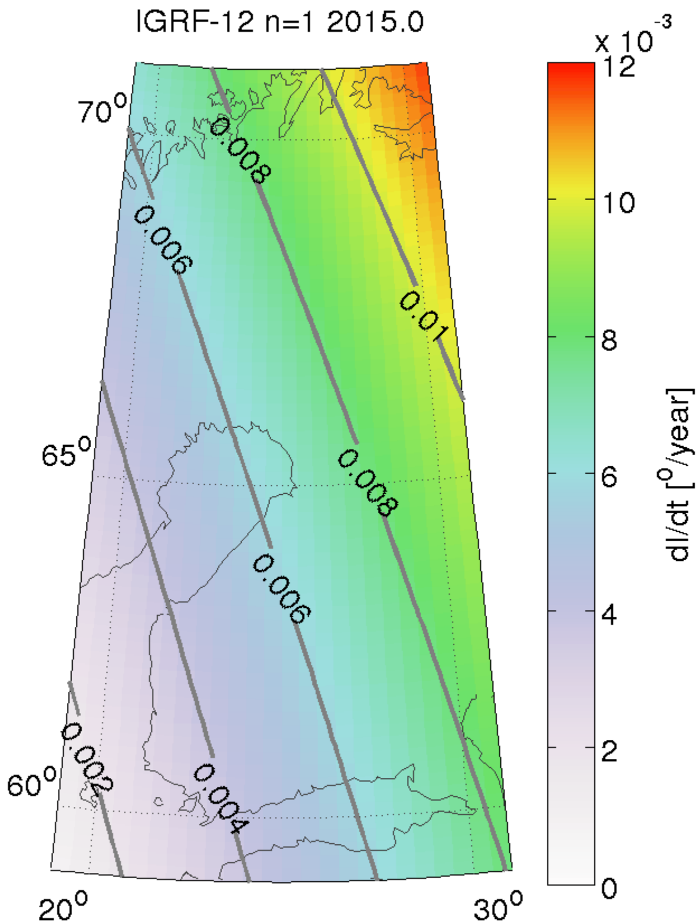
IGRF-12 n=1 2015.0
x 10-3
12
10
8
6
4
2
0
dI/dt [o/year]
70o
65o
60o
20o
30o
0.002
0.004
0.006
0.008
0.01

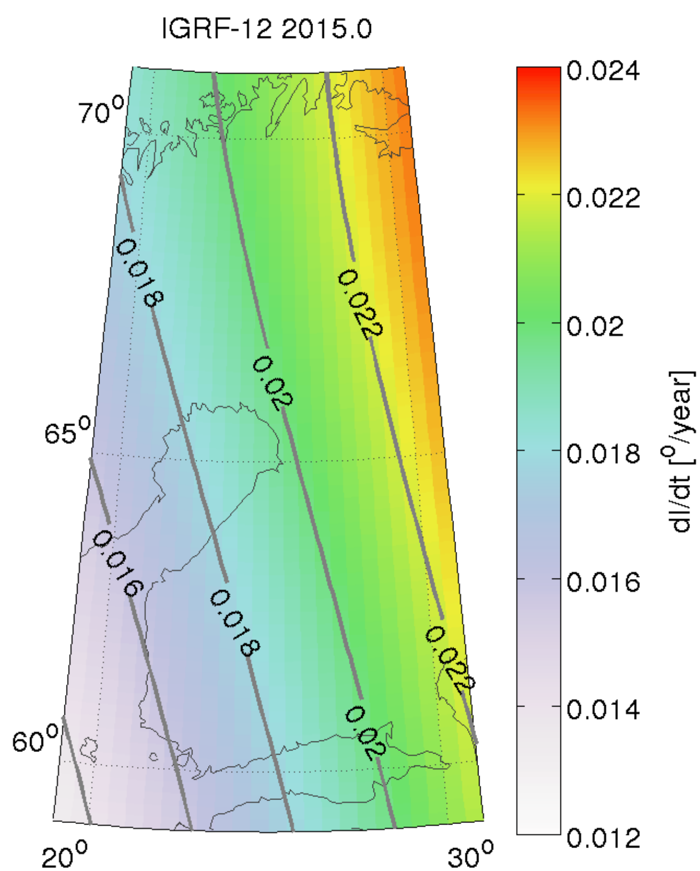
IGRF-12 2015.0
0.024
0.022
0.02
0.018
0.016
0.014
0.012
dI/dt [o/year]
70o
65o
60o
20o
30o
0.016
0.018
0.02
0.022

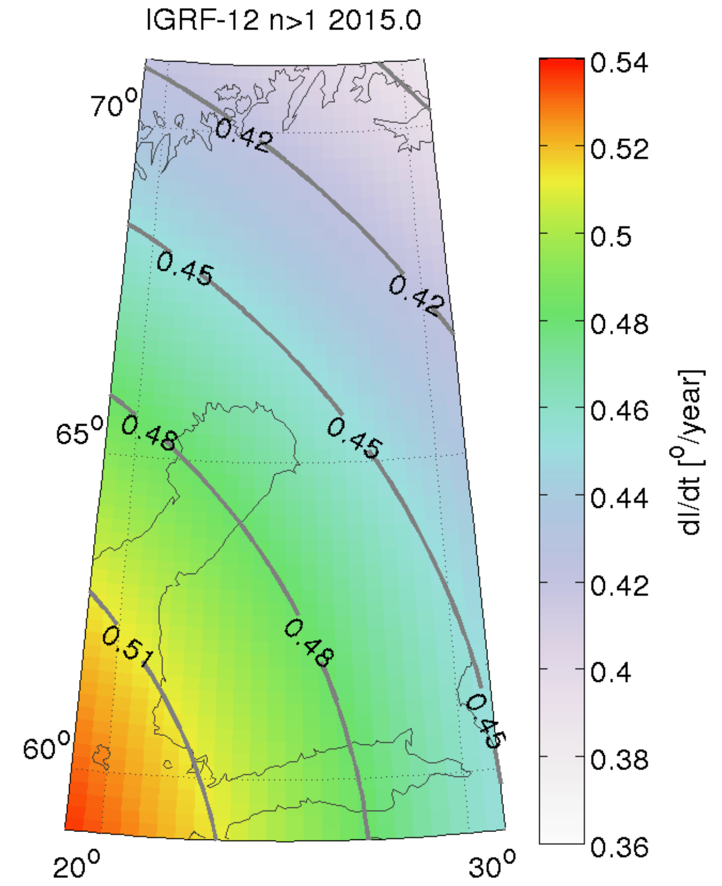
IGRF-12 n>1 2015.0
0.54
0.52
0.5
0.48
0.46
0.44
0.42
0.4
0.38
0.36
dI/dt [o/year]
70o
65o
60o
20o
30o
0.42
0.45
0.48
0.51

Altitude-Adjusted Corrected Geomagnetic Coordinates (AACGM)

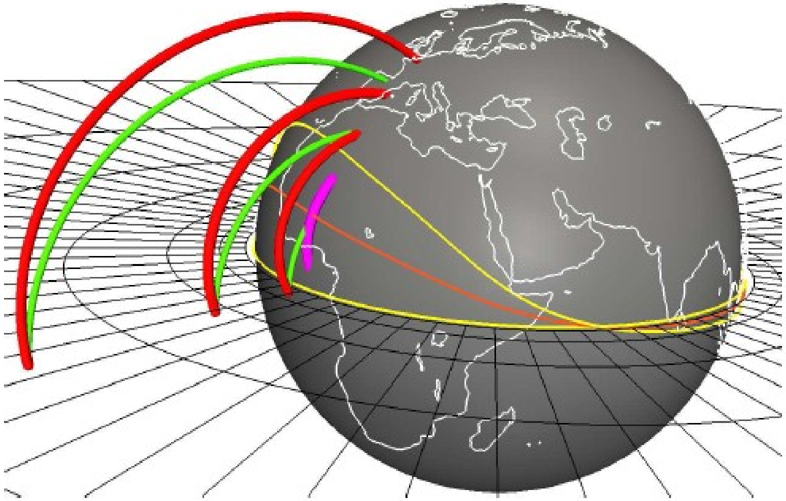

Examples of determining AACGM coordinates for four geographic locations along the prime meridian. Red lines represent IGRF field lines emanating from geographic starting locations at 50º, 40º, 30º latitude, and ending at the Earth-centered magnetic dipole equator. AACGM coordinates are given by the coordinates of the dipole field lines, shown in green. The magenta line shows the IGRF field line starting at 20º latitude, which intersects the surface of Earth before the dipole equator. AACGM coordinates are undefined for such locations. The region near the magnetic dip equator (orange line) which includes these field lines is marked by yellow lines on Earth's surface. From: Shepherd (2014).